PREPARATION AND SOLID STATE PROPERTIES OF CYCLODEXTRIN COMPLEXES OF SELECTED DRUG MOLECULES

BY

EINO NATANGWE MVULA

B.Sc. (University of Namibia)

B.Sc. (Honours) (University of Cape Town)

Thesis presented to the

UNIVERSITY OF CAPE TOWN

for the degree of

MASTER OF SCIENCE

Department of Chemistry

University of Cape Town

Rondebosch

7701

South Africa

March 1999

ACKNOWLEDGEMENTS

I would like to thank:

- Associate Professor Mino R. Caira for his time, patience and excellent supervision
- Dr Susan A. Bourne for her kind help and valuable comments
- my parents for their love and support
- my friends for keeping me company during the write up
- members of the crystallography research group for their friendship and good sense of humour
- and the University of Namibia for financial support.

PUBLICATIONS AND CONFERENCES

Parts of this thesis are currently in press:

M. R. Caira, S. A. Bourne and E. N. Mvula, Thermoanalytical study of the dehydration of cyclodextrin complexes of clofibric acid, *J. Therm. Anal.*, accepted February 1999.

Parts of this thesis have been presented at the following conferences:

1. M. R. Caira, S. A. Bourne and E. N. Mvula, Solid state properties of β- and γ-cyclodextrin complexes of clofibric acid, Poster no.59, Presented at the 19th Annual Conference of the Academy of Pharmaceutical Sciences, 28 June – 1 July 1998, Durban, South Africa.
2. M. R. Caira, S. A. Bourne and E. N. Mvula, Thermoanalytical study of the dehydration of cyclodextrin complexes of clofibric acid, Poster no. 2/P-5, Presented at the 7th European Symposium on Thermal Analysis and Calorimetry, 30 August – 4 September 1998, Balatonfüred, Hungary.

ABSTRACT

A large number of pharmaceutically important drugs are poorly soluble in water. This study focuses on the 'smart' molecule that can enhance the solubility and hence increase the bioavailability of these drugs. This molecule is a cyclodextrin and is known to form inclusion compounds with various drug molecules.

The preparation of β-cyclodextrin (β-CD), γ-cyclodextrin (γ-CD), heptakis(2,6-di-*O*-methyl)-β-cyclodextrin (Dimeb) and heptakis(2,3,6-tri-*O*-methyl)-β-cyclodextrin (Trimeb) complexes with clofibric acid as well as the heptakis(2,3,6-tri-*O*-methyl)-β-cyclodextrin (Trimeb) complex with clofibrate is reported. The complexes were characterised by thermogravimetric analysis (TG), differential scanning calorimetry (DSC), ultraviolet spectrophotometry (UV), infrared spectroscopy (IR), X-ray powder diffraction (XRD) and single crystal X-ray analysis.

Infrared spectroscopy for the four inclusion complexes of clofibric acid showed a significant shift of the C=O stretching frequency in the complexed drug relative to the uncomplexed drug.

The crystal structures of the complexes, except that of the Dimeb complex with clofibric acid, were solved. The guest molecules in the β- and γ-CD complexes were found to be disordered, preventing detailed interpretation of the mode of inclusion. The guest molecules in the two Trimeb complexes were resolved and the modes of inclusion were revealed. The aliphatic chains of the guests were found to be inserted in the cavity, while the chlorophenyl rings protrude from the secondary side of the Trimeb molecule. Kinetics of dehydration studies for β- and γ-CD complexes of clofibric acid, as well as for their

corresponding hosts were carried out. Attempts were made to correlate the kinetic behaviour with the crystal structures of these compounds.

In addition, solubility studies carried out on two benzodiazepine drugs (alprazolam and midazolam) in randomly methylated β-CD (Rameb) and 2-hydroxypropyl-β-CD (2-HP β-CD) solutions showed a significant solubility enhancement factor. Attempts to prepare solid cyclodextrin complexes of alprazolam and midazolam proved to be unsuccessful as expected from phase solubility studies. The crystal structure of midazolam sesquihydrate prepared from aqueous solution by the pH adjustment method was solved.

ABBREVIATIONS AND SYMBOLS USED IN THE TEXT

α	extent of reaction
A	Arrhenius pre-exponential factor
α-CD	α-cyclodextrin
β-CD	β-cyclodextrin
β_{nm}	Overall stability constant for the n:m complex
CD	cyclodextrin
CETMB	Trimeb complex of clofibrate
COBCD	β-cyclodextrin complex of clofibric acid
CODMB	Dimeb complex of clofibric acid
COGCD	γ-cyclodextrin complex of clofibric acid
COTMB	Trimeb complex of clofibric acid
CSD	Cambridge Structural Database
D_c	calculated density for the crystal
Dimeb	heptakis(2,6-di-*O*-methyl)-β-cyclodextrin
DSC	differential scanning calorimetry
E_a	activation energy
$f(\alpha)$	kinetic rate expression
F_c	calculated structure factor
F_o	observed structure factor
γ-CD	γ-cyclodextrin
2-HPβ-CD	2-hydroxypropyl β-cyclodextrin
IR	infrared spectroscopy

k	rate constant
K_{nm}	stepwise stability constant for the n:m complex
$[L_o]$	initial concentration of the complexing agent
$[L_t]$	total concentration of the complexing agent
M_r	molecular weight
NMR	nuclear magnetic resonance spectroscopy
Rameb	randomly methylated β-CD
$[S_o]$	concentration of the solute in the absence of the complexing agent
$[S_t]$	total concentration of the solute
TG	thermogravimetric analysis
T_{on}	onset temperature
Trimeb	heptakis(2, 3, 6-tri-*O*-methyl)-β-cyclodextrin
UV	ultraviolet spectroscopy/ spectrophotometry
V	unit cell volume
XRD	X-ray powder diffraction
Z	number of molecules in the unit cell

TABLE OF CONTENTS

ACKNOWLEDGEMENTS i
PUBLICATIONS AND CONFERENCES ii
ABSTRACT iii
ABBREVIATIONS AND SYMBOLS USED IN THE TEXT v
TABLE OF CONTENTS vii

CHAPTER 1: INTRODUCTION
1.1 CYCLODEXTRINS 1
1.2 CYCLODEXTRIN COMPLEXES 3
1.3 PROPERTIES OF CDS AND THEIR COMPLEXES IN SOLUTION 4
1.3.1 SOLUBILITY OF COMPLEXES 4
1.3.1.1 THEORY OF PHASE SOLUBILITY STUDIES 4
1.3.1.2 SOLUBILITY DATA OF CD-DRUG SYSTEMS 9
1.4.1 NMR STUDIES 11
1.5 SOLID STATE PROPERTIES OF CD COMPLEXES 12
1.5.1 THERMAL ANALYSIS 12
1.5.1.1 DIFFERENTIAL SCANNING CALORIMETRY (DSC) AND THERMOGRAVIMETRIC ANALYSIS (TG) 12
1.5.1.2 THERMAL DEHYDRATION KINETICS 13
1.5.2 CRYSTAL STRUCTURE 15
1.5.2.1 MOLECULAR CONFORMATION OF CDs AND THEIR COMPLEXES 15
1.5.2.2 MOLECULAR PACKING OF CDs AND THEIR COMPLEXES 17
1.6 MOTIVATION AND OBJECTIVES OF THE STUDY 23
1.7 REFERENCES 26

CHAPTER 2: EXPERIMENTAL
2.1 MATERIALS 32
2.2 PREPARATION OF COMPLEXES 32
2.3 THERMAL ANALYSIS 33
2.3.1 THERMOGRAVIMETRIC ANALYSIS (TG) AND DIFFERENTIAL SCANNING CALORIMETRY (DSC) 33
2.3.2 ISOTHERMAL TG 33
2.4 ULTRAVIOLET SPECTROPHOTOMETRY (UV) 34
2.5. INFRARED SPECTROSCOPY(IR) 35
2.6 X-RAY POWDER DIFFRACTION (XRD) 35

2.7 CRYSTAL STRUCTURE ANALYSIS 35
2.8 COMPUTATION 36
2.8.1 CRYSTAL STRUCTURE DETERMINATION AND REFINEMENT 36
2.8.2 MOLECULAR AND CRYSTAL PACKING 37
2.8.3 CALCULATED XRD PATTERN 38
2.9 REFERENCES 39

CHAPTER 3: β- AND γ-CYCLODEXTRIN COMPLEXES OF CLOFIBRIC ACID
3.1 INTRODUCTION 40
3.2 PREPARATION OF COMPLEXES 41
3.3 THERMAL ANALYSIS 41
3.4 STOICHIOMETRY OF THE COMPLEXES 43
3.5 INFRARED SPECTROSCOPY (IR) 43
3.6. X-RAY POWDER DIFFRACTION 43
3.7 CRYSTAL STRUCTURE 45
3.7.1 DATA-COLLECTION 45
3.7.2 COBCD COMPLEX 45
3.7.2.1 STRUCTURE DETERMINATION AND REFINEMENT 45
3.7.2.2 HOST-GUEST INTERACTION AND CRYSTAL PACKING 48
3.7.2.3 CONFORMATION OF THE HOST MOLECULE 52
3.7.3 COGCD COMPLEX 54
3.7.3.1 STRUCTURE DETERMINATION AND REFINEMENT 55
3.7.3.2 HOST-GUEST INTERACTION AND CRYSTAL PACKING 55
3.7.3.3 CONFORMATION OF THE HOST MOLECULE 58
3.8. KINETICS OF DEHYDRATION 60
3.8.1 RESULTS FOR THE KINETICS OF DEHYDRATION 61
3.8.2 KINETICS OF DEHYDRATION IN RELATION TO CRYSTAL STRUCTURE 64
3.9 REFERENCES 66

CHAPTER 4: DIMEB AND TRIMEB COMPLEXES OF CLOFIBRIC ACID
4.1 INTRODUCTION 68
4.2 THERMAL ANALYSIS 68
4.3 STOICHIOMETRY OF THE COMPLEXES 71
4.4 INFRARED SPECTROSCOPY (IR) 71

4.5 X-RAY STRUCTURE ANALYSIS 72
4.5.1 DATA-COLLECTION 72
4.5.2 STRUCTURE DETERMINATION AND REFINEMENT 72
4.5.3 HOST-GUEST INTERACTION AND CRYSTAL PACKING 76
4.5.4 CONFORMATION OF THE HOST MOLECULE 79
4.5.5 CONFORMATION OF THE GUEST MOLECULE 80
4.6 X-RAY POWDER DIFFRACTION 83
4.7 REFERENCES 86

CHAPTER 5: TRIMEB COMPLEX OF CLOFIBRATE
5.1 INTRODUCTION 87
5.2 PREPARATION OF THE COMPLEXES 88
5.3 THERMAL ANALYSIS 88
5.4 SINGLE CRYSTAL STRUCTURE ANALYSIS 89
5.4.1 DATA-COLLECTION 89
5.4.2 STRUCTURE DETERMINATION AND REFINEMENT 90
5.4.3 HOST-GUEST INTERACTION AND CRYSTAL PACKING 91
5.4.4 CONFORMATION OF THE HOST MOLECULE 95
5.4.5 CONFORMATION OF THE GUEST MOLECULE 97
5.5 X-RAY POWDER DIFFRACTION 98
5.6 REFERENCES 100

CHAPTER 6: CYCLODEXTRIN INCLUSION OF BENZODIAZEPINES
6.1 INTRODUCTION 101
6.2 SOLUBILITY STUDIES 103
6.2.1 METHODOLOGY 103
6.2.2 PHASE DIAGRAMS AND STABILITY CONSTANTS FOR MIDAZOLAM 103
6.2.3 PHASE DIAGRAMS AND STABILITY CONSTANTS FOR ALPRAZOLAM 106
6.3 CD COMPLEXES OF BENZODIAZEPINES 108
6.4 THERMAL ANALYSIS OF MIDAZOLAM SESQUIHYDRATE 109
6.5 CRYSTAL STRUCTURE OF MIDAZOLAM SESQUIHYDRATE 110
6.5.1 DATA-COLLECTION 110
6.5.2 STRUCTURE DETERMINATION AND REFINEMENT 101
6.5.3 CRYSTAL PACKING OF MIDAZOLAM SESQUIHYDRATE 113
6.5.4 CONFORMATION OF MIDAZOLAM 115
6.6 REFERENCES 117

CHAPTER 7: CONCLUSION

7.1 CONCLUSION 117

7.2 REFERENCES 121

APPENDICES

APPENDIX A 122

APPENDIX B 122

CHAPTER ONE

CHAPTER 1: INTRODUCTION

1.1 CYCLODEXTRINS

The products of starch digestion by *Bacillus macerans* are known as cyclodextrins. These molecules were discovered by Villiers [1] in 1891 and were fully characterised by Schardinger.[2] The structure of cyclodextrins (CDs) only came to be known 40 years after their discovery when Freudenberg et al. came to the conclusion by using data published by Karrer,[3] and Miekeley,[4] that the cyclodextrins are made up of glucose units with a α-1,4 glycosidic linkages as shown in Fig 1.1(a). The structure of α-D glucose is shown in Fig 1.1(b). The digestion of starch *by Bacillus macerans* yields three different products which are systematically named as α-, β-, and γ-CD. The three products differ in that they are made of 6, 7 and 8 α-D glucose units respectively as shown in Fig 1.2. The differences in the numbers of glucose units in the ring give rise to differences in both physical and chemical properties of the cyclodextrins. One of the differences in physical properties is the solubility in the aqueous solution. The solubilities of the native CDs increase in the order β- < α– < γ-CD. The differences in the numbers of glucose units also give rise to differences in the radii of the macrocycles and the number of water molecules per CD molecule. The radii of the cavities are 5.7, 7.8 and 9.5 Å for α-, β-, and γ-CD and the crystal water contents at high humidity are 6.6, 12 and 17 water molecules per α-, β-, and γ-CD molecule respectively. [5,6]As shown in Fig 1.2, the glucose unit of the CD has hydroxyl groups on C(2), C(3) and C(6) which are accessible to functional group transformation.[7-9] A number of CD derivatives can be made by changing the functional groups at these positions. Only the β–CD derivatives are discussed here.

The common β–CD derivatives are heptakis(2,6-di-*O*-methyl)-β–CD (Dimeb), heptakis(2,3,6-tri-*O*-methyl)- β–CD (Trimeb), randomly methylated β–CD (Rameb) and 2-hydroxypropyl β–CD (2-HPβ–CD). Dimeb and Trimeb are crystalline while Rameb and 2-HPβ–CD are amorphous. These β–CD derivatives have high aqueous solubility as well as greater ability to form inclusion complexes than their parent hosts. The solubilities of the methylated β–CD derivatives decrease with increase in temperature, while the hydroxypropylated derivatives follow a similar solubility pattern to the native CDs.

CDs and their derivatives play a very important role in drug formulations in that they can be used to (1) stabilise drugs that are light or air sensitive, (2) improve dissolution rates and bio-availability of drugs, (3) reduce side effects and other unfavourable properties. [5,6,10]

The toxicity profiles as well as the metabolic fate of cyclodextrins have been thoroughly investigated and well documented.[5,6,11,12] It is believed that native CDs are quite safe for oral administration as most of the CDs are degraded by intestinal flora in the colon. The relative amounts of undegraded CD that are absorbed into the bloodstream are less than 2, 6 and 0.1 percent for α-, β- and γ-CD respectively. Parenteral administration of native CDs and methylated CD derivatives results in haemolysis of the erythrocytes;[11,12] therefore such administration should be limited to 2-hydroxypropyl β–CD.

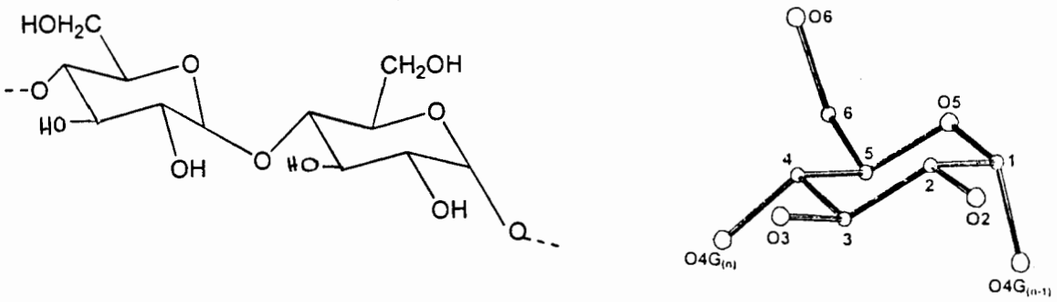

(a) (b)

Figure 1.1 (a) Two glucose units linked by α-1,4 glycosidic bond (a) Structure of glucose unit with the numbering scheme (H atoms are omitted)

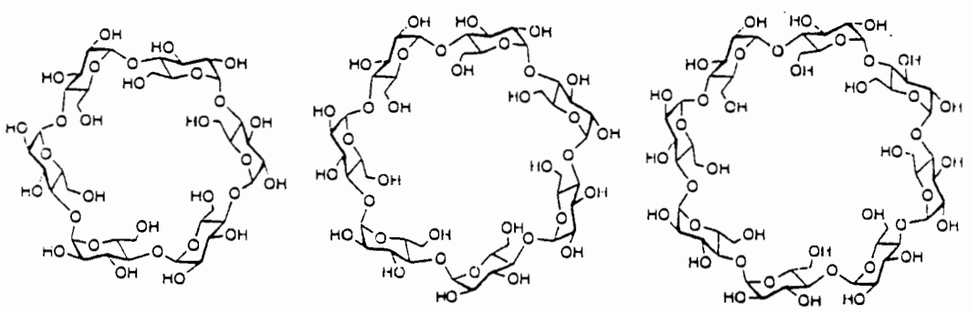

α β γ

Figure 1.2 α-, β-, and γ-cyclodextrin

1.2 CYCLODEXTRIN COMPLEXES

Cyclodextrins are capable of forming inclusion complexes with various guest molecules having a size compatible with the dimension of the CD cavity.[5] The following methods are used for the synthesis of cyclodextrin complexes:

(1) Kneading: in which the CD is kneaded with a small amount of water followed by the addition of an appropriate amount of guest, (2) Co-grinding: this involves vigorous grinding of the CD and the guest drugs without addition of any solvent, and

(3) Co-precipitation: here both drug and CD are stirred together in solution, preferably using water as a solvent.[6,13]

Depending on the properties of the guest molecules, complexes may or may not be formed using either of the preparation methods discussed above. Based on statistical data on the complexes published so far, supramolecular chemists were able to postulate the following essential conditions for complex formations:[5,14,15]

- The size and the shape of the guest molecules- the size of the guest molecule must be compatible with the diameter of the cavity
- The properties of the guest molecule- the guest molecule should be hydrophobic as the interior of the cavity is hydrophobic.

1.3. PROPERTIES OF CDs AND THEIR COMPLEXES IN SOLUTION

1.3.1 SOLUBILITY OF COMPLEXES

This section will cover the theory of the phase solubility technique and its application to CD complexes.

1.3.1.1 THEORY OF PHASE SOLUBILITY TECHNIQUE

The classical review of phase solubility techniques by Higuchi and Connors[16] has sparked a major experimental gathering of information on phase solubility studies. Such techniques are applied to various systems including the drug-CD system.

Solubility measurements are generally carried out by adding an excess amount of solute (S) into several containers (normally flasks) containing different known concentrations of a complexing agent (L). The samples are brought to equilibrium by shaking and then analysed for their concentration of S by suitable means.

The construction of what is known as phase solubility diagrams facilitates the analysis of solubility data. The phase solubility diagram is a plot of the total concentration of S in the solution vs. the concentration of L. The phase diagrams are classified into two classes, the A type (the solubility of S is increased by the presence of L) and the B type as shown in Figure 1.3. The A type diagrams are further subdivided into the following:

- A_L- This is observed if complexes of first order in L are formed e.g. SL, S_2L,...,S_mL
- A_P- This is observed as a result of higher order complexes in L e.g. SL_2, SL_3,...,SL_n
- A_N- the physical meaning of a type A_N diagram is unclear.

The B type diagrams are subdivided into:

- B_S –This indicates the formation of a soluble complex which eventually reaches its solubility-limit and further addition of L results in the depletion of S from solution,

B_I- Insoluble complex formed.[16, 17]

The general chemical equation for the host-guest interaction can be written as follows:

$$mS + nL \Leftrightarrow L_nS_m \qquad 1.1$$

At equilibrium, the overall stability constants for the interaction can be defined as [18]

$$\beta_{nm} = \frac{[L_nS_m]}{[L]^n[S]^m} \qquad 1.2$$

where β_{nm} is the overall stability constant, $[L_nS_m]$ is the concentration of the complex formed, $[L]$ and $[S]$ are concentrations of complexing agent (ligand) and solute respectively. The overall stability constant β_{nm} is also related to the stepwise stability constants K by the following expression:

$$\beta_{nm} = \prod_m \prod_n K_{nm} \qquad 1.3$$

The total concentrations of each species in the reaction vessel can be expressed as

$$L_t = [L] + \sum_n \sum_m n[L_n S_m] \qquad 1.4$$

$$S_t = [S_o] + \sum_n \sum_m m[L_n S_m] \qquad 1.5$$

In the equations above L_t and S_t are the total concentrations of L and S respectively. S_o is the concentration of S in the absence of L. L_t and S_t are related to the overall stability constants by rewriting equations 1.4 and 1.5 as follows:

$$L_t = [L] + \sum_n \sum_m n\beta_{nm}[L]^n[S]^m \qquad 1.6$$

$$S_t = [S_o] + \sum_n \sum_m m\beta_{nm}[L]^n[S]^m \qquad 1.7$$

The general expression given forms the basis for the analysis of phase solubility diagrams as well as the calculation of the stability constants.

A_L diagrams

As mentioned earlier, A_L type diagrams are observed when complexes of first order with respect to L are formed. [17-26] In that case the overall equations 1.2, 1. 6 and 1. 7 can be rewritten as:

$$\beta_{1m} = \frac{[LS_m]}{[L]\ [S]^m} \qquad 1.8$$

$$L_t = [L] + \sum_1 \sum_m \beta_{1m}[L]\ [S]^m \qquad 1.9$$

$$S_t = [S_o] + \sum_1 \sum_m m\beta_{1m}[L]\ [S]^m \qquad 1.10$$

Equations 1.9 and 1.10 can be combined to yield a linear relationship between S_t and L_t.

$$S_t = \frac{\sum m\beta_{1m}[S_o]_m}{1+\sum \beta_{1m}[S_o]} L_t + [S_o] \qquad 1.11$$

A plot of S_t vs. L_t is linear with slope $\frac{\sum m\beta_{1m}[S_o]_m}{1+\sum \beta_{1m}[S_o]}$; for a 1:1 complex the slope is equal to $\frac{K_{11}[S_o]}{1+K_{11}[S_o]}$

AP diagrams

The A_P diagrams occur when complexes of higher order with respect to L are formed. For the purpose of calculating the stability constants, it is common practice to describe the A_P diagrams by assuming that only SL and SL_2 complexes are formed. Based on the assumption described above, the total concentration of S and L in the reaction vessel can be expressed by equations 1.12 and 1.13 respectively

$$S_t = [S_o] + K_{11}[S_o][L] + K_{11}K_{12}[S_o][L]^2 \qquad 1.12$$

$$L_t = [L] + K_{11}[S_o][L] + 2K_{11}K_{12}[S_o][L]^2 \qquad 1.13$$

Subtracting 1.12 from 1.13 followed by rearrangement yields the following :

$$[L] = \frac{Q}{1-K_{11}[S_o]} \qquad 1.14$$

where $Q = L_t - 2(S_t - [S_o])$ 1.15

If equation 1.14 is substituted into equation 1.12 and the resulting expression divided by Q, a linear relationship between $\frac{S_t - [S_o]}{Q}$ and Q is obtained.

The y-intercept of such a plot is $c = \frac{K_{11}[S_o]}{1-K_{11}[S_o]}$ 1.16

and the gradient is given by $m = \frac{cK_{12}Q}{1-K_{11}[S_o]}$ 1.17

Both K_{11} and K_{12} can be calculated from equations 1.16 and 1.17.

Type B diagram

The calculation of the stability constants from the ascending part of the B_S diagram is similar to that for the type A diagrams. The descending part of both B_S and B_I can also be used to calculate the stability constants. In this case a certain stoichiometry of the complex is assumed in order to calculate the stability constants (K_{mn}) from the data available. On the B diagrams there are two points which are useful for calculating K_{nm} (see Fig 1.4): point A which is a point of inflection and B, the solubility limit of the complex.[16,17]

The stability constant for an n:m complex is given by

$$K_{nm} = \frac{[S_B]}{[S_x - mS_B]^m [L_x - nS_B]^n} \qquad 1.18$$

where $[S_x]$ and$[L_x]$ are the concentrations of solute and complexing agent respectively at point x and are calculated by equations 1.19 and 1.20:

$$[S_x] = [S] + m[S_m L_n] \qquad 1.19$$

$$[L_x] = [L] + n[S_m L_n] \qquad 1.20$$

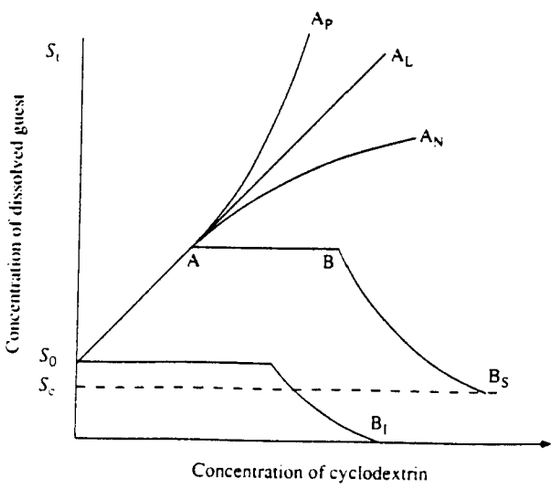

Figure 1.3 Phase solubility diagrams

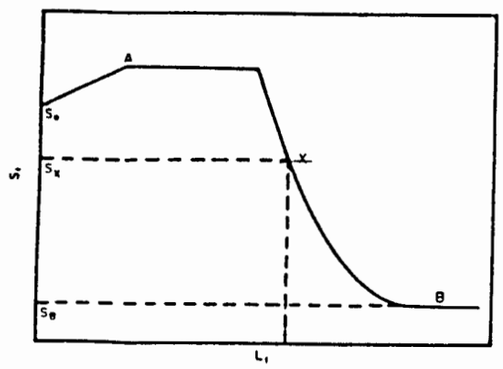

Figure 1.4 Type B diagram showing calculation of the stability constants

1.3.1.2 SOLUBILITY DATA OF CD-DRUG SYSTEMS

There is a vast number of publications dedicated to CD-drug systems.[19-52] This section merely gives a representation of some of the data. Table 1.1 shows the magnitude of interaction between CDs and some guest molecules.

Table 1.1: Drug-CD interactions in solution derived from phase solubility diagrams

Guest	*Host*	*Diagram Type*	*Stability constant* $K_{1:1}$ $[M^{-1}]$	$K_{1:2}$ $[M^{-1}]$	*References*
4-biphenyl acetic acid	β-CD				27
	HPβ-CD				
	Dimeb				
	Trimeb				
	β-CD	A_L	1190±105		28
tolnaftate	HPβ–CD(3%)	A_P	1460±139		
	HPβ–CD(8%)	A_P	1860±165		
hydrocortisone	β–CD	B_S	4792	1739	29
psoralen	β-CD	A_L	663		30
	Dimeb	A_L	603		
	Trimeb	A_L	69.6		
oxazepam	β-CD	A_L	205		31
pregnanolone	HPβ-CD	A_P			32
pilocarpine	HPβ-CD	A_p			33
	α–CD	B_S			
	β-CD	B_S			
	γ-CD	B_S			34
Alkannin /shikonnin enantiomers	HPβ-CD	A_L	260.5		35

Table 1.1 Continued

Anandamide	HPβ-CD	A_P	39419	12	36
(arachidonyl	Dimeb	A_L	74487		
ethanolamide)	HPγ-CD	A_L	15469		
furosemide	β-CD	B_S	823.5		37
clofibrate	β-CD	B_S	1315		38
	HPβ-CD	A_L			
	Dimeb	A_L			
propanidid	HPβ-CD	A_L			39
19-norprogesterone	β-CD	A_L			25
	HPβ-CD	A_L			
	HEβ-CD	A_L			
miconazole	α-CD	A_L	333		40
	β-CD	A_L	293		
	γ-CD	A_L	695		
	HPβ-CD	A_L	363		
	HEβ-CD	A_L	305		
haloperidol	Dimeb	A_L	2435		41
	HPβ-CD	A_L	2112		
triamterene	β-CD	A_L	340		42
ketoconazole	β-CD	A_L			43
	HPβ-CD	A_L			
gliclazide	β-CD	B_S	1094		44
naproxen	α-CD	A_L	40		45
	β-CD	A_L	1702		
	γ-CD	A_L	146		
	HPα-CD	A_L	103		
	HPβ-CD	A_L	283		
	HPγ-CD	A_L	187		
salicylic acid	β-CD	B_S	666		46
nifedipine	β-CD	A_L	77.9		22
	γ-CD	A_P	53.1	3.5	
	Dimeb	A_P	283.1	11.3	
	Rameb	A_P	184.9	5.8	
	2HPβ-CD	A_L	77.2		
	2HPγ-CD	A_L	49.3		
furosemide	β-CD	B_S			47
	HPβ-CD	A_L			
	Rameb	A_L			
	Dimeb	A_L			
manidipine	β-CD	B_S			23
	γ-CD	A_L			
	Rameb	A_P			
	Dimeb	A_P			
triflumizole	β-CD	A_L		470	48

1.5 SOLID STATE PROPERTIES OF CD COMPLEXES

1.5.1 THERMAL ANALYSIS

Thermal analysis has been used in order to describe properties of many solid substances. In the pharmaceutical industry thermal analysis is used to measure thermal stability and the presence of volatile material in the sample. This section presents the thermal analytical techniques used to study CD complexes and the properties which are likely to be observed.

1.5.1.1 DIFFERENTIAL SCANNING CALORIMETRY (DSC) AND THERMOGRAVIMETRIC ANALYSIS (TG)

TG gives quantitative data for loss of mass as a function of temperature and DSC measures the amount of heat evolved or released by the sample during a temperature programme.

CDs and their complexes generally lose their water contents below 100 °C. The water loss (dehydration) from the CD or CD complexes are characterised by endothermic peaks on the DSC traces in the region of 30 to 100 °C.[5] Both TG and DSC serve very important purposes in helping to characterise inclusion complexes. TG is mostly used to determine the water content of the CD or CD complexes. True inclusion complexes can be distinguished from a physical mixture of host and guest by DSC because the guest molecule is often retained in the host cavity until the CD decomposes.[5,6]

The native CDs and their complexes decompose above 250 °C while the methylated derivatives such as Trimeb and Dimeb decompose at around 200 °C.

1.5.1.2 THERMAL DEHYDRATION KINETICS

Solid state reactions are characterised by the breaking down of one or more components into simpler atomic groupings.[62] The general equation for the solid state reaction can be written as:

$$A_{(s)} \rightarrow B_{(s)} + C_{(g)} \qquad 1.21$$

Cyclodextrin molecules and their complexes crystallise as hydrates; upon heating, water is released in the form of vapour. The decomposition reaction of CDs and their respective complexes can be represented by equations 1.22 and 1.23 respectively.

$$CD \cdot nH_2O_{(s)} \rightarrow CD_{(s)} + nH_2O_{(g)} \qquad 1.22$$

$$CD \cdot G \cdot nH_2O_{(s)} \rightarrow CD \cdot G_{(s)} + nH_2O_{(g)} \qquad 1.23$$

Solid state kinetics of dehydration studies are carried out using thermogravimetric analysis.[63] There are two thermogravimetric methods that are used in studying reaction kinetics, namely isothermal and non-isothermal gravimetry. These methods are well developed and there are several reviews and monographs on this subject.[62-66] In this section only the isothermal gravimetric analysis is described. The interpretation of kinetic data is facilitated by the use of the Arrhenius equation:

$$k = A\exp(-E_a/RT) \qquad 1.24$$

where A is the pre-exponential factor, k is the rate constant, R is the gas constant, T is the temperature and E_a is the activation energy. The most important parameter in equation 1.24 is the activation energy.[66] The kinetic studies involve the measurement of $\alpha = \frac{m_t - m_o}{m_f - m_o}$ as a function of time at a constant temperature. α is known as the

extent of reaction while m_t, m_o and m_f are the mass of the sample at time t, initial mass and final mass respectively. The rate laws for solid state reactions in the integral form can be written as:

$$f(\alpha) = kt \qquad 1.25$$

Table 1.2 shows the kinetic models which describe $f(\alpha)$ and these models are used to determine the mechanisms of the reaction. The determination is done by plotting $f(\alpha)$ vs. time using the α-time data. The model which gives the best linear fit is chosen to be the correct one.

Table 1.2: Theoretical kinetic models for solid-gas reactions

	$f(\alpha) = kt$
1. Acceleratory α-time curves	
P1 power law	$\alpha^{1/n}$
E1 exponential law	$ln\alpha$
2. Sigmoid α-time curves	
A2 Avrami-Erofe'ev	$[-ln(1-\alpha)]^{1/2}$
A3 Avrami-Erofe'ev	$[-ln(1-\alpha)]^{1/3}$
A4 Avrami-Erofe'ev	$[-ln(1-\alpha)]^{1/4}$
B1 Prout-Tompkins	$ln[\alpha/(1-\alpha)]$
3. Deceleratory α-time curves	
3.1 based on geometrical models	
R2 contracting area	$1-(1-\alpha)^{1/2}$
R3 contracting sphere	$1-(1-\alpha)^{1/3}$
3.2 based on diffusion controlled models	
D1 one-dimensional	α^2
D2 two-dimensional	$(1-\alpha)ln(1-\alpha)+\alpha$
D3 three-dimensional	$[1-(1-\alpha)^{1/3}]^2$
D4 Ginstling-Brounshtein	$(1-2\alpha/3)-(1-\alpha)^{2/3}$
3.3 based on "order of reaction"	
F1 first order	$-ln(1-\alpha)$
F2 second order	$1/(1-\alpha)$
F3 third order	$[1/(1-\alpha)]^2$
Fn n-th order	$[1/(1-\alpha)]^n$

The application of kinetics studies to cyclodextrins is still in its infancy.

Szafranek et al.[67-70] have carried out studies on β-CD hydrate, β-CD deuterate and β-CD complexes. These authors have used non-isothermal gravimetric methods. It was found that the dehydration process for the β-CD hydrate followed a zero order mechanism with an activation energy of 65 kJ mol^{-1}.[67]

1.5.2 CRYSTAL STRUCTURE

1.5.2.1 MOLECULAR CONFORMATION OF CYCLODEXTRINS AND THEIR COMPLEXES

As previously stated in Section 1.1, CDs consist of α-D glucose units in a $^4C_1$ conformation. The atoms in the glucose unit are numbered as shown in Fig 1.1(b). In this section the structures of β-CD, its methylated derivatives (Dimeb and Trimeb) and γ-CD are discussed. Generally, the O(2) and the O(3) atoms of the adjacent glucose units in a CD molecule form intramolecular hydrogen bonding, which results in the stability and rigidity of the macrocycle. There are various geometric parameters which are used to define the CD conformation namely:[71]

- Planarity of the O(4) polygon, the root-mean-square deviation of O(4) from the least-squares plane.
- Tilt angle, the angle made by the least-squares plane through the O(4) atoms and a plane through C(1), C(4), O(4) and O(4') of each glucose residue.
- Torsion angle index: this measures the differences in conformation of each glucose unit and changes associated with complex formation.
- The O(4)···O(4') distances: these give a measure of distances between the O(4) atoms of the adjacent glucose units.

- Glycosidic angle: this defines the angle subtended at the O(4) atom i.e the angle $C(4G_n)$-$O4G_n$-$C(1G_{n+1})$.
- The O(2)···O(3') distances are characteristic of intramolecular hydrogen bonding in native CDs which maintains the round structure of the macrocycle. In Trimeb these distances are longer because there is no possibility of hydrogen bonding (see Table 1.3).[72]
- Radius of the O(4) polygon: the average value of the distance from the centre of the polygon to each O(4) atom.

All the above geometric parameters for β-CD, γ-CD, Dimeb and Trimeb are listed in Table 1.3.

Table 1.3 :Geometrical data for cyclodextrin macrocycles: distances (Å) and angles (°)

Parameter	β-CD[73]	γ-CD[74]	Dimeb[75]	Trimeb[76]
Tilt angle (°)	14(10)	19(9)	14(8)	20(25)
Glycosidic angle (°)	118(1)	117(1)	117(1)	117(2)
planarity of the O(4) polygon (Å)	0.16	0.09	0.44	0.11
Radius of the O(4) polygon (Å)	5.0(0.2)	5.9(0.1)	5.1(0.2)	5.0(0.3)
O(2)···O(3') distance (Å)	2.9(0.1)	2.8(0.1)	2.9(0.1)	3.5(0.2)
O(4)···O(4') distance (Å)	4.3(0.1)	4.5(0.1)	4.4(0.1)	4.3(0.1)

It is evident from the list of parameters that each macrocycle has unique geometric properties. The average radii of the polygons increase as the number of glucose units in the ring increases.

1.5.2.2 MOLECULAR PACKING OF CDs AND CD COMPLEXES

Different CDs and their complexes have different crystal packing modes. In this section the packing modes of β-CD, γ-CD, Dimeb and Trimeb are discussed.

β-Cyclodextrin

β-Cyclodextrin and its complexes crystallise in the following different packing modes:

- *Cage-type packing*

Cage-type packing (see Fig 1.5) has been observed in β-CD dodecahydrate, as well as in β-CD complexes with small guest molecules such as ethanol,[77] ethylene glycol,[78] hydrogen iodide[79] and methanol.[79] All of the above mentioned complexes crystallise in the monoclinic space group $P2_1$. In β-CD dodecahydrate, 6.5 of the 12 H_2O molecules are located in the cavity and the guest molecules in all other complexes are included in the cavity together with some water molecules. The β-CD molecules are packed along a 2-fold screw-axis resulting in a herringbone like structure; hence this packing mode is also referred to as 'herringbone'.[80] In this packing arrangement, either side of the CD molecule is blocked by part of an adjacent CD molecule and the guest as well as the water molecules in the cavity are completely isolated.

- *Channel-type packing*

In this type of arrangement, β-CD complexes form head-to-head dimers as shown in Fig.1.6. The channel type complexes belong to one of the space groups P1, C2 or $P2_1$. The dimer unit in space group P1 or C2 forms a linear endless channel. A zigzag channel is observed in crystals with space group $P2_1$. β-CD complexes which pack in

a linear channel include those of benzocaine,[81] m-iodobenzoic acid,[82] 3,3-dimethylbutylamine,[83] p-nitroacetanilide and many others. β-CD complexes with carmofur,[84] iodoaniline, o-ethylaniline [85] and benzil [86] pack in a zigzag channel mode. Many of the channel β-CD complexes which crystallise in the space group C2 contain disordered guests.

- *Layer-type packing*

The layer-type packing (Fig 1.7) is observed when the guest molecule is too large to be fully enclosed in the cavity. All of the β-CD complexes which form layer packing crystallise in the space group $P2_1$, for example β-CD with triethylenediamine[84] and sulfathiazole.[87] In this type of arrangement both ends of the β-CD cavity are closed by parts of the adjacent β-CD molecules. There are also some layer structures which are composed of head-to-head dimer units of β-CD. This has been observed in the β-CD complex with 4-*tert*-butylbenzyl alcohol which crystallises in the space group $C222_1$.[74] The bulk of the guest molecule is fully immersed in the cavity with its hydroxymethyl group protruding from the primary end of the cavity and forming intermolecular hydrogen bonding with the β-CD molecule of the next layer. In this case both ends of the cavity are open to the intermolecular space of the next layer.

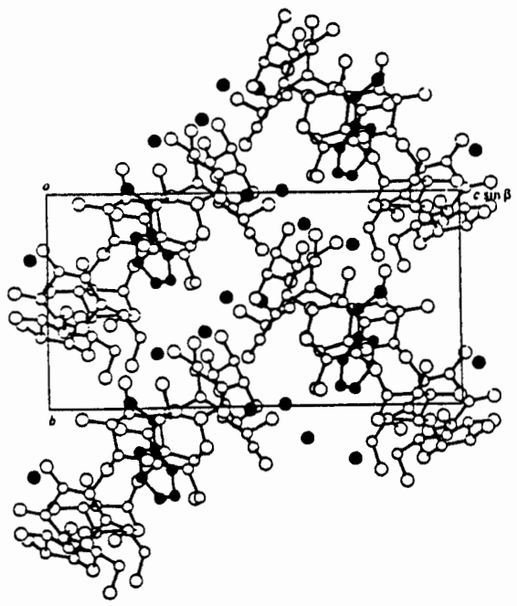

Figure 1.5 Cage-type packing found in the β-CD complex with benzyl alcohol.[71]

(•) represent atoms of the guest and water molecules

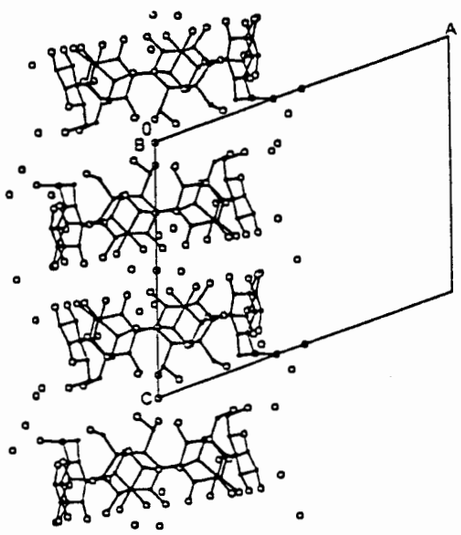

Figure 1.6 Channel packing arrangement found in the β-CD complex with ibuprofen. A view down [010].[96] Open circles represent oxygen atoms of the host and water molecules

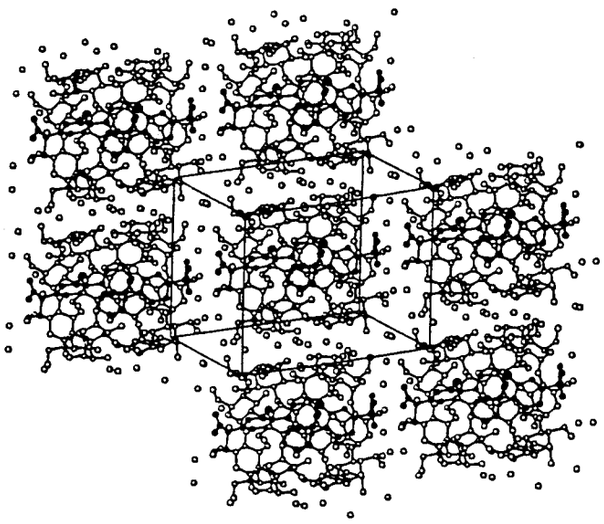

Figure 1.7: Layer-type packing found in the β-CD complex with (S)-flurbiprofen.[71]

(•) represent atoms of the guest molecules

γ-Cyclodextrin

γ-CD and its complexes crystallise in two crystal forms, namely cage- and channel-type. The only known cage-type structure of γ-CD is a hydrate which crystallises in the monoclinic space group $P2_1$.[70] In a complexed form, γ-CD crystallises in a channel-type structure in which case the CD molecule is situated on a 4-fold rotation axis parallel to the unique axis *c*, as shown in Figure 1.8. The inside of the cavity is large and the included guest molecules experience diffusive motions. Both the 4-fold symmetry and the diffusion motion contribute to the statistical disorder of the guest molecules in the CD cavity making it difficult to model the guest. There are a few crystal structures of γ-CD complexes in which the guest is fully resolved from X-ray diffraction data, for example γ-CD·12-crown-4·Li and γ-CD·12-crown-4·K complexes.[88]

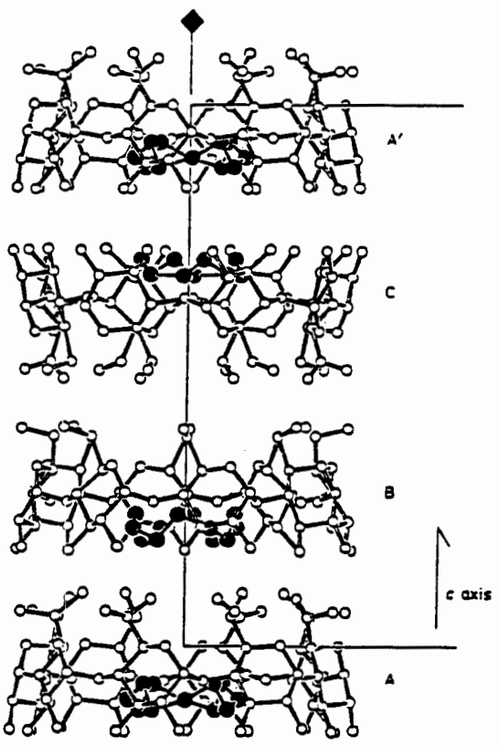

Fig 1.8: The channel structure of γ-CD-12-crown-4-inclusion complex.[88]

(•) represent atoms of the guest molecules

Dimeb

Dimeb and its complexes known so far crystallise in the orthorhombic space group $P2_12_12_1$. The structure of Dimeb exhibits a round macrocyclic conformation which is maintained by intramolecular O(3)-H····O(2) hydrogen bonding. There are very few Dimeb complex crystal structures reported because it is very difficult to obtain crystals of good quality for X-ray diffraction. The molecular packing of the Dimeb complexes with the following guests is discussed: 2-naphthoic acid [89] p-iodophenol and p-nitrophenol.[75] In the structure of the Dimeb complex with 2-naphthoic acid, the guest molecule is inserted in the cavity with its carboxylic group protruding from the O(6) side of the Dimeb molecule. This complex molecule packs in exactly the same

way as the uncomplexed Dimeb. It is surprising to note that the guest molecules in Dimeb complexes with both p-iodophenol and p-nitrophenol are not located in the cavity but rather in the interstitial sites, as shown in Figure 1.9. This led to the conclusion that the intermolecular space in the crystal structure is hydrophobic.[80]

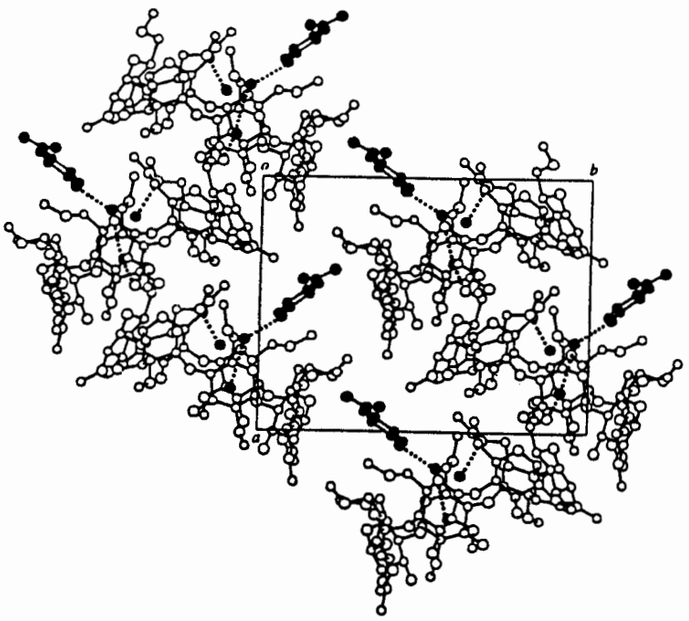

Fig 1.9 Crystal structure of Dimeb complex with p-nitrophenol.[75]

(•) represent guest atoms and water molecules

Trimeb

Like Dimeb, Trimeb and its complexes crystallise in the space group $P2_12_12_1$, but nevertheless the crystal modes of packing of these complexes differ significantly. All Trimeb complexes tend to form head-to-head packing modes giving rise to a zigzag channel-type structure as shown in Figure 1.10. The channels lie on a 2-fold screw axis. The guest molecules are never fully immersed in the Trimeb cavity, a large portion of the guest often protruding from the O(2), O(3) side of the macrocycle.

This has been observed in many of the structures of complexes reported in literature e.g biphenylacetic acid,[90] flurbiprofen,[91] naproxen,[92] ibuprofen[93] and p-iodophenol.[94]

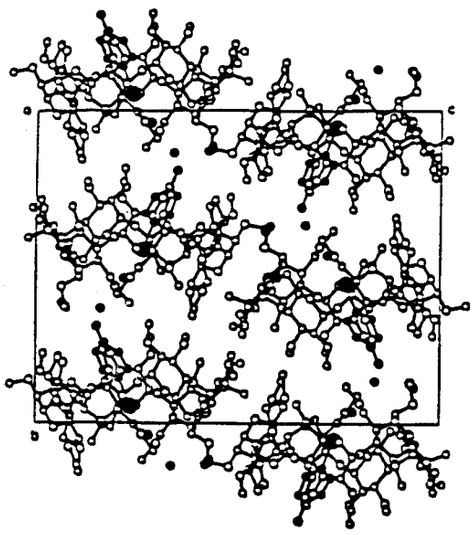

Figure 1.10 Crystal structure of Trimeb with p-iodophenol.[94]

(•) reperesent guest atoms and water molecules

1.6 MOTIVATION AND OBJECTIVES OF THE STUDY

The pharmaceutical industry has been experiencing a number of problems related to the unfavourable properties of some drugs, such as adverse side effects (e.g. gastrointestinal irritation) and poor aqueous solubility. In recent years the industry has turned to a "wonder molecule", namely cyclodextrin, with the aim of improving the properties of some pharmaceutically important drugs.

Although it has been known for a long time that cyclodextrins can form inclusion complexes with various pharmaceutical compounds, the structural information gathered so far offers very little when it comes to systematising the nature and the driving forces of complex formation. It is usually difficult to predict the space group

in which the complex crystallises and the mode of host-guest interaction from the structure of the drug and that of a cyclodextrin, except in the case of γ-CD where all complexes thus far investigated crystallise in the tetragonal space group $P42_12$. Therefore, one of the aims of this project is to contribute to the database of CD inclusion complexes which could be used to formulate the theory of CD-drug interaction.

The host CD molecules used in this project were β-CD, γ-CD, Trimeb, Dimeb, Rameb and 2-HPβ-CD. The drug molecules chosen for this project were two anti-hyperlipoproteinemic drugs clofibric acid (I) and clofibrate (II), an anxyolitic drug alprazolam (III), and an anaesthetic drug midazolam (IV). Preliminary phase solubility studies were carried out to establish whether the delivery properties of midazolam and alprazolam could benefit from CD complexation.

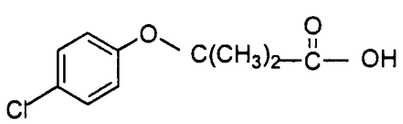

I

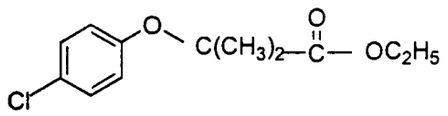

II

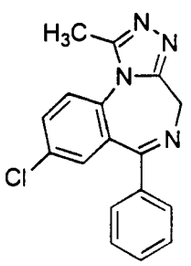

III

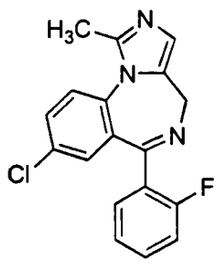

IV

Both midazolam and alprazolam are benzodiazepine molecules. There are a number of publications on the CD inclusion of benzodiazepine molecules, based on NMR and

molecular mechanics studies.[26,95] However, there are no detailed crystallographic data on such complexes. Therefore attempts were made to prepare single crystals of such complexes suitable for X -ray analysis.

In this project we emphasise the preparation and characterisation of the complexes prepared. The techniques employed in characterising the complexes are DSC, TGA, X-ray powder diffraction (XRD), ultraviolet spectroscopy (UV), infrared spectroscopy (IR) and single crystal X-ray studies.

By characterising the complexes and solving the crystal structures one can obtain the following vital information:

- Thermal stability of the complexes.
- The mode of host-guest interaction.
- Conformation of the included guest molecule.
- The spatial distribution of water molecules in the crystal structure.
- The parameters obtained from single crystal X-ray analysis can be used to calculate idealised XRD patterns which in turn are useful as standard references for comparison with experimental XRD patterns from bulk quantities of complexes prepared in the pharmaceutical industry.

Another area of interest which is addressed here is the study of the kinetics of dehydration which can give information on the stability of the hydrated complexes. Such studies are carried out using isothermal methods of analysis. The kinetic parameters, in favourable cases, can be correlated with the structure of the complexes obtained from X-ray analysis. This is indeed a useful means of elucidating the dynamic process of the solid state reaction.

1.7 REFERENCES

1. A. Villiers, *Compt. Rend. Acad. Sci.*, 1891, **112**, 536.

2. F. Z. Schardinger, *Unters. Nahr. u. Genussm.*, 1903, **6**, 865.

3. P. Karrer, *Helv .Chim. Acta*, 1921, **4**, 169.

4. A. Miekeley, *Ber. Dtsch. Chem. Ges.*, 1932, **65**, 69.

5. K. -H. Frömming and J. Szejtli, *Topics in Inclusion Science-Cyclodextrins in Pharmacy*, Kluwer Academic Publishers, Dordrecht, 1994.

6. J. Szejtli, *Topics in Inclusion Science-Cyclodextrins in Pharmacy*, Kluwer Academic Publishers, Dordrecht, 1988.

7. M. I. Bender and M. Komoyama, *Cyclodextrin Chemistry, Springer-Verlag*, New York, 1978.

8. J. Szejtli, *Supramolecular Chem.*, 1995, **6**, 217.

9. J. Szejtli, *J. Incl. Phenom.*, 1992, **14**, 25.

10. S. P. Jones, D. J. W. Grant, J. Hadgraft and G. D. Part, *Acta Pharm. Techno.*, 1984, **30**, 213.

11. D. O. Thompson, CRC *Crit. Rev. Ther. Drug Carrier Syst.*, 1997, **14**, 1.

12. T. Irie, M. Sunada, M. Otagiri, K. Uekama, Y. Ohtani, Y. Yamada and Y. Sugiyama, *J. Pharmacobi-Dyn.*, 1982, **5**, 741.

13. A. L. Hedges, *Chem. Rev.*, 1998, **98**, 2035.

14. K. Harata, *Bull. Chem. Soc. Jpn.*, 1982, **55**, 1367.

15. K. Harata, *J. Chem. Soc., Chem. Commun.*, 1993, 546.

16. T. Higuchi and K. Connors: *Adv. Anal. Chem. Inst.*, 1965, **4**, 147

17. M. B. Zughul and A. A. Badwan, *J. Incl. Phenom.*, 1998, **31**, 243.

18. K. Iga, A. Hussain and J. Kashira, *J. Pharm. Sci.*, 1981, **70**, 108.

19. M. B. Maurin, S. M, Rowe, C. A. Koval and M. A. Hussain, *J. Pharm. Sci.*, 1994, **83**, 1418.

20. M. B. Zughul and A. A. Badwan, *Int. J. Pharm.*, 1997, **151**, 109.

21. T. Loftsson and M. E. Brewster, *J. Pharm. Sci.*, 1996, **85**, 1017.

22. M. S. Worthington, B. D. Glass, L. J. Penkler, *J.Incl. Phenom.*, 1996, **25**, 153.

23. K. Csabai, M. Vikmon, J. Szejtli, E. Redenti, G. Poli and P. Ventura, *J. Incl. Phenom.*, 1998, **31**, 169.

24. P. Montassier, D. Duchêne and M. C. Poelman; *J. Incl. Phenom.*, 1998, **31**, 213.

25. S. M. Ahmed, *J. Incl. Phenom.*, 1998, **30**, 111.

26. S. A. Andronati, Y. E. Shapiro, L. N. Yakubovskaya, V. Y. Gorbatyuk, K. S. Andronati, and S. P. Krasnoschekaya, *J. Incl. Phenom.*, 1996, **24**, 175.

27. C. A. Ventura, G. Puglisi, G. Giammona and F. A. Bottino, *Drug Dev. Ind. Pharm.*, 1994, **20**, 2245.

28. D. Peri, C. M. Wyandt, R. W. Cleary, A. H. Aikal, and A. B. Jones, *Drug Dev. Ind. Pharm.*, 1994, **20**, 1401.

29. A. Preiss, W. Mehnret and K. H. Frömming, *Archive Der Pharmazie*, 1994, **327**, 729.

30. F. F. Vincieri, G. Mazzi, N. Mulinacci, M. Bambagiotti, F. Dallacqua, and D. Vedaldi, *Il Farmaco*, 1995, **50**, 543.

31. J. R. Moyano, M. J. Arias, J. M. Gines and A. M. Rabasco, *Int. J. Pharm.*, 1998, **114**, 95.

32. M. E. Brewster, W. R. Anderson, T. Loftsson, M. J. Huang, N. Bodor and E. Pope, *J. Pharm. Sci.*, 1995, **85**, 1154.

33. P. Jarho, A. Urtti and T. Jarvinen, *Pharm. Res.*, 996, **137**, 209.

34. S. Ito, M. Demachi, Y. Toriumi, T. Adachi, S. Itai, F. Hirayama and K. Uekama, *Chem. Pharm. Bull.*, 1995, **43**, 2221.

35. C. Y. Chen, F. A. Chen, A. B. Wu, H. C. Hsu, J. J. Kang, H. W. Cheng, *Int. J. Pharm.*, 1996, **141**, 171.

36. P. Jarho, A. Urtti, D. W. Pate, P. Suhonen and T. Jarvinen, *Int. J .Pharm.*, 1996 **137**, 209.

37. N. Ozdemir and S. Ordu; *Drug Dev. Ind. Pharm.*, 1998, **24**, 19.

38. S. Aguiano-Igea, F. J. Otero-Espinar, J. L. Vila-Jato, J. Blanco-Méndez, *Eur. J. Pharm. Sci.,* 1997, **5**, 215.

39. C. R. Mackenzie, J. P. Fawcett, C. W. Boulton and I. G. Tucker, *Int. J. Pharm.*, 1997, **159**, 191.

40. S. Tenjari, P. Puranajoti, R. Kasina and T. Mandal; *J. Pharm. Sci.*, 1998, **87**, 425.

41. Y. L. Loukas, V. Vraka and G. Gregoriadis, *J. Pharm. and Biomed. Anal.,* 1997, **16**, 263.

42. M. J. Ariasblanco, J. R. Mayano and J. M. Gines, *Int. J. Pharm.,* 1996, **153**, 181.

43. M. T. Vila-Jato and J. J. Torres-Labandeira, *Int. J. Pharm.*, 1996, **143**, 203.

44. J. R. Mayano, M. J. Ariasblanco, J. M. Gines, J. I. Perezmartinez, G. Bettinetti and F. Giordano, *J. Pharm. Sci.,* 1997, **86**, 72.

45. F. Melani, G. P. Bettinetti, P. Mura and A. Monderioli, *J. Incl. Phenom.,* 1995, **22**, 131.

46. D. Chow and A. Karata, *Int. J. Pharm.*, 1986, **28**, 95.

47. R. M. Amin Kreaz, G. Y. Dombi and M. Kata, *J. Incl. Phenom.*, 1998, **31**, 189.

48. C. T. Klein, G. Köhler, B. Mayer, K. Mraz, S. Recter, H. Viernstein and P. Wolschann, *J. Incl. Phenom.*, 1995, **22**, 15.

49. K. K. Chacko and W. Saenger, *J. Am. Chem Soc.*, 1981, **103**, 1708.

50. H. Ueda and T. Nagai, *Chem. Pharm. Bull.*, 1980, **28**, 1415.

51. H. Ueda and T. Nagai, *Chem. Pharm. Bull.*, 1981, **29**, 2710.

52. D. Djedaïni and B. Perly, In *New Trends in Cyclodextrins and Derivatives,* Chapter 6, *ED.*, D. Duchene, Editions de Santé, Paris, France, 1991.

53. P. V. Dermarco and A. L. Thakka, *J. Chem. Soc., Chem. Commun.*, 1970, 2.

54. R. Fornassier, V. Lucchini, P. Srimin and U. Tonnelato, *J. Incl. Phenom.*, 1986, **4**, 292.

55. S. Li and W. C. Purdy, *Anal. Chem.*, 1992, **B4**, 1405.

56. Z. Li, Q. Guo, T. Ren, X. Zhu and Y. Liu, *J. Incl. Phenom.*, 1993, **15**, 359.

57. M. E. Amato, G. A. Pappalardo and B. Pertly, *Magnetic Resonance in Chemistry,* 1993, **31**, 455.

58. M. E. Amato, F. Djedaini-Pilard, B. Pertly and G. Scarlatta, *J. Chem. Soc., Perkin Trans. 2,* 1992, 2065.

59. G. Fronza, A. Mele, E. Redenti and P. Ventura, *J. Org. Chem.*, 1996, **616**, 909.

60. J. R. Mayano, M. J. Ariasblanco, J. M. Gines and F. Giordano, *Int. J. Pharm.*, 1997, **157**, 239.

61. J. R. Mayano, M. J. Ariasblanco, J. M. Gines, J. I. Perezmartinez, G. Bettinetti and F. Giordano, *J. Incl. Phenom.*, 1996, **25**, 137.

62. C. H. Bamford and C. F. H. Tipper, *Comprehensive Chemical Kinetics,* Volume 22, Elsevier, Amsterdam, 1980.

63. D. Dollimore, *Thermal Analysis- Techniques and Applications,* Eds., E.L. Charsley and S. B. Warrington, Royal Society of Chemistry, Cambridge, 1992.

64. M. E. Brown, *Introduction to Thermal Analysis - Technique and Applications* Chapmann and Hall, London, 1988.

65. W. M. Wendlandt, *Thermal Analysis*, John Wiley and Sons, New York, 1964.

66. D. Dollimore, *Thermochim. Acta*, 1992, **7**, 203.

67. A. Szafranek, *J. Thermal. Anal.*, 1988, **34**, 917.

68. A. Szafranek and J. Szafranek, *J. Incl. Phenom.*, 1993, **15**, 351.

69. A. Szafranek and J. Szafranek, *J. Incl. Phenom.*, 1998, **30**, 163.

70. J. H. Li, N. Zhang, X. T. Li, J. Y. Wang, *J. Incl. Phenom.*, 1997, **28** ,95.

71. K. Harata, *Comprehensive Supramolecular Chemistry*, Vol.3, eds., J. L. Atwood, J. E. Davies and D. MacNicol, Oxford University Press, New York, 1991.

72. K. Harata, *Bull. Chem. Soc. Jpn.*, 1987, **60**, 2763.

73. K. Lindner and W. Saenger, *Carbohydr. Res.*, 1982, **99**, 103.

74. D. Mentzafos, I. M. Mavridis, G. Les Bas and G. Tsoucaris, *Acta Crystallogr.*, 1991, **B47**, 746.

75. K. Harata, *Bull. Chem. Soc. Jpn.*, 1988, **61**, 1939.

76. K. Harata, *J. Chem. Soc.,Chem. Commun.*, 1988, 928.

77. R. Tokuoka, M. Abe, T. Fujiwara, K. Tomita and W. Saenger, *Chem. Lett.*, 1980, 491.

78. K. Gessler, T. Steiner and W. Saenger, *Carbohydrate Res.*, 1993, **249**, 327.

79. K. Harata, *Carbohydrate Res.*, 1982, **107**, 7.

80. K. Harata, *Chem. Rev.*, 1998, **98**, 1803.

81. J. Hamilton and M. N. Sabesa, *Carbohydrate Res.*, 1982, **102**, 31.

82. J. Hamilton, M. N. Sabesa and L. Steinrauf, *Carbohydrate Res.*, 1981, **89**, 33.

83. I. M. Mavridis and Hadjoudis, *Carbohydrate Res.*, 1992, **229**, 1.

84. K. Harata, F. Hirayama and G. Tsoucaris, *Chem. Lett.,* 1988, 1585.

85. R. Tokuoka, T. Fujiwara and K. Tomita, *Acta Crystallogr.,* 1981, **B37**, 1158.

86. G. Les Bas, C. De Rango, N. Rysanek and G. Tsoucaris, *J. Incl. Phenom.*, 1985, **2**, 861.

87. M. R. Caira, V. J. Griffith and L. R. Nassimbeni, *J. Incl. Phenom.*, 1994, **17**, 187.

88. S. Kamitori, K. Hirotsu and K. Higuchi, *J. Am. Chem. Soc.*, 1987, **109**, 2409.

89. K. Harata, *Bull. Chem. Soc. Jpn.*, 1990, **63**, 2481.

90. K. Harata, F. Hirayama, H. Arima and K. Uekama, *J. Chem. Soc., Perk. Trans. 2,* 1992, 1159.

91 K. Harata, F. Hirayama, K. Uekama and M. Otagiri, *J. Incl. Phenom.*, 1988, **6**, 443.

92. M. R. Caira, V. J. Griffith, L. R. Nassimbeni and B. van Oudtshoorn, *J. Incl. Phenom.*, 1995, **20**, 277.

93. G. R. Brown, M. R. Caira, L. R. Nassimbeni and B. van Oudtshoorn, *J. Incl. Phenom.*, 1996, **26**, 281.

94. K. Harata, K. Uekama, M. Otagiri and F. Hirayama, *Bull. Chem. Soc. Jpn.,* 1983, **56**, 1732.

95. U. Uekama, S. Narisawa, F. Hirayama and M. Otagiri, *Int. J. Pharm.,* 1987, **16**, 327.

96. G. R. Brown, *The Physicochemical Characterisation of Cyclodextrin Inclusion Compounds with Non-steroidal Anti-inflammatory Drugs*, MSc Thesis, University of Cape Town, 1997.

CHAPTER TWO

CHAPTER 2: EXPERIMENTAL

2.1 MATERIALS

The host compounds β-cyclodextrin, γ-cyclodextrin, Trimeb, Dimeb, Rameb and HPβ-CD were obtained from Cyclolab, Hungary, and were used as received.

The guest compounds clofibric acid and clofibrate were purchased from Sigma Chemical Co., Missouri, USA, while alprazolam and midazolam were obtained from South African Druggists International, Port Elizabeth, South Africa.

2.2 PREPARATION OF COMPLEXES

All complexes, except where otherwise stated, were prepared by the co-precipitation method which involved the addition of equimolar amounts of drug and CD to water. For the preparation of β-cyclodextrin and γ-cyclodextrin complexes, the drug was added to a CD solution and the mixture was stirred for 12 h at 65 °C. Single crystals of these compounds were then obtained by filtering the hot solution with microfilters whose pore size was 0.45μm and allowing the solutions to evaporate. Single crystals grew in two to three days.

Dimeb and Trimeb complexes were prepared by stirring the CD and drug solution at room temperature for 4 h. Their single crystals were prepared by filtering the solution with a 0.45 μm microfilter followed by elevating the temperature of the solution to 50 °C in a tank with thermostatic control. The crystals were formed within a day.

2.3 THERMAL ANALYSIS

2.3.1 THERMOGRAVIMETRIC ANALYSIS (TG) AND DIFFERENTIAL SCANNING CALORIMETRY (DSC)

TG experiments are carried out to determine the weight loss of a sample as a function of temperature, when the sample is heated at a constant rate. The DSC experiments measure the enthalpy changes occurring when the inclusion compounds undergo dehydration, phase change or melt. These experiments were performed on a Perkin Elmer PC7 system. The scans were carried out at a heating rate of 10 °C min^{-1} under nitrogen gas purge with a flow rate of 30 ml min^{-1}. The masses of the samples were in the range 3-5 mg and the programmed temperature runs were between 30 and 350 °C, unless otherwise stated. Samples for the TG runs were placed in open aluminium pans while vented aluminium pans were used for DSC samples.

2.3.2 ISOTHERMAL TG

Isothermal thermogravimetric experiments were also carried out to determine the kinetics of dehydration for selected CD complexes. This was performed on the PC7 system by rapidly heating the sample to a required temperature in the range 35-70 °C. Samples used in this experiment were microcrystalline powders with particle size in the range of 10-100μm, obtained by complex crystallisation from rapidly stirred solutions. Mass losses measured with time were used to obtain α (extent of reaction) vs. time curves which were analysed using kinetic models[1] to seek the best linear fits over the α-range of 0.05-0.95.

2.4. ULTRAVIOLET SPECTROPHOTOMETRY (UV)

Since cyclodextrins are UV inactive, UV plays an essential role in determining the amount of drug present in a specific mass of the sample or in the CD solution, provided the drug has an appropriate UV spectrum. In this study UV was used for determining the stoichiometry of the prepared complexes as well as for the phase solubility studies.

- Determination of complex stoichiometry

The stoichiometry was determined in conjunction with the TG results. A known mass of the sample was dissolved in a water-ethanol solution (40:60 by volume) followed by the measurement of the absorbance. The concentration of the drug in the solution was calculated using the Beer-Lambert law, which in turn determines the percentage content of the drug in a specific sample.

- Phase solubility studies

Phase solubility studies were carried out to measure the effect of cyclodextrin on the solubility of the drug. The measurements of the amount of drug dissolved in a CD solution were done using UV spectrophotometry. This topic is discussed in detail in Chapter 6. Absorbance measurements were performed on a Philips PU8700 UV/vis spectrophotometer in the range 200-400 nm at scanning rate of 200 nm min^{-1}.

2.5 INFRARED SPECTROSCOPY (IR)

The formation of an inclusion compound is known to have an effect on the spectroscopic properties of the guest molecule.[2,3] Such effects can be evaluated by comparing the spectroscopic properties of pure drug to that of the complexed drug. In this study IR was used to determine the effect of CD complexation on the C=O stretching frequency of some guest molecules. Infrared spectra were recorded on a Perkin Elmer 983 IR spectrophotometer. Samples were prepared by grinding the material in nujol mull® and then placing the mull between two sodium chloride plates.

2.6 X-RAY POWDER DIFFRACTION (XRD)

XRD patterns were recorded on a Philips PW1050/80 vertical goniometer equipped with a PW1394 motor control unit. Ni-filtered CuKα radiation (λ= 1.5418Å), generated by a Philips PW1130/90 generator, was used. The samples were packed into aluminium sample holders and scanned over the 2θ range of 6-40° at intervals of 0.1° with 2s counts.

2.7. CRYSTAL STRUCTURE ANALYSIS

Single crystals of suitable size (between 0.2 and 0.5 mm in all dimensions) were selected for diffractometry experiments on the basis of their ability to extinguish plane-polarised light uniformly. All crystals were mounted onto glass fibres using cyanoacrylate adhesive. Unstable crystals, such as those of complexes with native cyclodextrins, were covered with cyanoacrylate to prevent decay due to the diffusion of water from the crystal.

Preliminary unit cell data and space group information were obtained from oscillation, Weissenberg and precession photographs taken on a Stoë goniometer using Ni-filtered CuKα radiation (λ= 1.5418Å), generated by a Philips PW1120 generator operating at 20mA and 40kV.

Data-collections were carried out on a Nonius Kappa CCD diffractometer, using graphite-monochromated MoKα radiation (λ= 0.71069Å). Most of the intensity data were recorded at 293K except those for CETMB, which were collected at 173 K. Details on the data-collection strategies are given for each structure in their respective chapters.

2.8 COMPUTATION

2.8.1 CRYSTAL STRUCTURE DETERMINATION AND REFINEMENT

All crystal structures of complexes were solved by isomorphous replacement methods using atomic co-ordinates for the non-hydrogen atoms of cyclodextrins in the isomorphous structures. The refinement was performed using SHELXL-93[4] which employs full-matrix least-squares refinement on F^2. The midazolam structure was solved by direct methods using program SHELXS-86[5] and the refinements were performed using the SHELXL-93[4] program. The reliability of the calculated structure model is measured by the *R*-factor. The values that will be quoted and which serve as a good measure for the reliability of the model are the residual index R_1, which is a measure of the agreement between the calculated (F_c) and observed (F_o) structure factors, and wR_2 based on the refinement on F^2.

These are given by

$$R_1 = \frac{\sum \| F_o | - | F_c \|}{\sum |F_o|}$$

$$wR_2 = \left(\frac{\sum w(F_o^2 - F_c^2)^2}{\sum w(F_o^2)^2} \right)^{1/2}$$

where w is the weight (a and b are refined for each structure)

$$w = 1/[\sigma^2(F_o^2) + (aP)^2 + bP]$$

$$P = [\max(0, F_o^2) + 2F_c^2]/3$$

The goodness of fit (S) based on F^2 serves as the basis for examining the analysis of variance for the F^2 values and is defined by:

$$S = \left[\frac{\sum [w(F_o^2 - F_c^2)^2}{n - p} \right]^{1/2}$$

where n is the number of reflections and p is the total number of refined parameters.

2.8.2 MOLECULAR AND CRYSTAL PACKING DIAGRAMS

Molecular and crystal packing diagrams were produced using a PC version of PLUTO.[6] The sizes of interstitial channels formed by the host were visualised using the program MOLMAP.[7] The Cambridge Structural Database (CSD)[8] was extensively used to obtain atomic co-ordinates of the structures which are isomorphous to those of complexes reported in this study as well as to compare structures of complexes with similar host molecules.

2.8.3. CALCULATED XRD PATTERN

The calculated XRD pattern was obtained using the program LAZYPULVERIX[9] running on a personal computer in a DOS environment. The space group data, unit cell parameters, co-ordinates of the atoms and their respective thermal parameters were used as input for the program.

2.9 REFERENCES

1. P. J. Haines, *Thermal methods of analysis,* Chapman and Hall, London, 1995.

2. K.-H. Frömming and J. Szejtli, *Topics in Inclusion Science-Cyclodextrins in Pharmacy*, Kluwer Academic Publishers, Dordrecht, 1994.

3. Y. C. Wei, A. M. Knevel, G. P. Carlson and C. J. Chang, *J. Incl. Phenom.,* 1996, **15**, 313.

4. G. M. Sheldrick, SHELXL-93, *Program for the Refinement of Crystal Structures*, University of Göttingen, Germany, 1993.

5. G. M. Sheldrick, *Acta Cryst.,* 1990, **A46**, 467.

6. W. D. S. Motherwell. PLUTO-89, *Program for plotting molecular and crystal structures*, University of Cambridge, 1989.

7. L. J. Barbour, *Clathration by Diol Hosts: Thermodynamics and Structure*, PhD Thesis, University of Cape Town, 1994.

8. Cambridge Structural Database and Cambridge Structural Database System, version 5.16, October 1998, Cambridge Crystallographic Data Centre, University Chemical Laboratory, Cambridge, England.

9. K. Yvon, W. Jeitschko and E. Parthe, *J. Appl. Crystallogr,* 1977, **10**, 73.

CHAPTER THREE

CHAPTER 3: β-AND γ–CD COMPLEXES OF CLOFIBRIC ACID

3.1 INTRODUCTION

The anti-hyperlipoproteinemic (cholesterol-lowering) drugs are among many pharmaceutical agents that are poorly soluble in water. Some studies on inclusion complexes of anti-hyperlipoproteinemic drugs have been reported.[1,2] Clofibrate and fenofibrate are two of the anti-hyperlipoproteinemic drugs that have been studied as guest molecules for complexation with CDs. Anguiano-Igea et al.[1] characterised the β-CD inclusion complex of clofibrate using XRD, DSC and IR spectroscopy. Although CD inclusion compounds were prepared and partially characterised, no single crystal X-ray studies were conducted on these inclusion complexes to establish the exact mode of inclusion. In this study, clofibric acid (I), that is 2-(4-chlorophenoxy)-2-methyl propionic acid, which is also poorly soluble in water, was investigated as guest molecule for inclusion into β-CD and γ-CD. Clofibric acid is an anti-hyperlipoproteinemic drug which is known to reduce triglyceride and cholesterol concentration in the serum.[3] It is also the active metabolite of clofibrate. Clofibric acid has been reported as crystallising in the monoclinic space group $P2_1/n$ where it occurs as hydrogen-bonded cyclic dimers.[4] This strong intermolecular hydrogen bonding results in poor solubility and slow dissolution rate, which are indeed the rate-limiting steps in gastro-intestinal absorption.

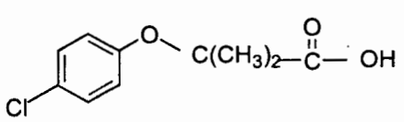

I

3.2 PREPARATION OF COMPLEXES

Complexes were prepared as described in section 2.2; here we report the characterisation of the β-CD and γ-CD complexes of clofibric acid, which will be referred to hereafter as COBCD and COGCD respectively.

3.3 THERMAL ANALYSIS

Both COBCD and COGCD were characterised by TG and DSC as described in section 2.3. The TG-DSC traces of COBCD and COGCD are shown in Figures 3.1 and 3.2 respectively. Characteristic DSC temperatures and estimated water contents from TG are listed in Table 3.1.

Table 3.1 TG-DSC data for COBCD and COGCD

Complex	Event (DSC)	Onset(T/ °C)	Peak (T/ °C)	%H_2O	H_2O molecules per CD molecule
COBCD	Endo A	48	66	10.1	8.4
	Endo B	104	110		
	Exo C	302	309		
COGCD	Endo A	50	75	15.6	15. 5
	Exo B	301	309		

Endo = endotherm; Exo = exotherm

The first stage in the decomposition of the complexes is dehydration which occurs from 40-99 °C. For COBCD, dehydration occurs in two steps as indicated by an inflection point on the TG trace and as distinct endotherms A and B in the DSC traces. This is followed by gradual mass loss with major decomposition occurring

exothermically from 299-329 °C (peak C). COGCD behaves similarly, except that what appears as a two-step process in TG is reflected only as a single endotherm (Peak A) in the DSC.

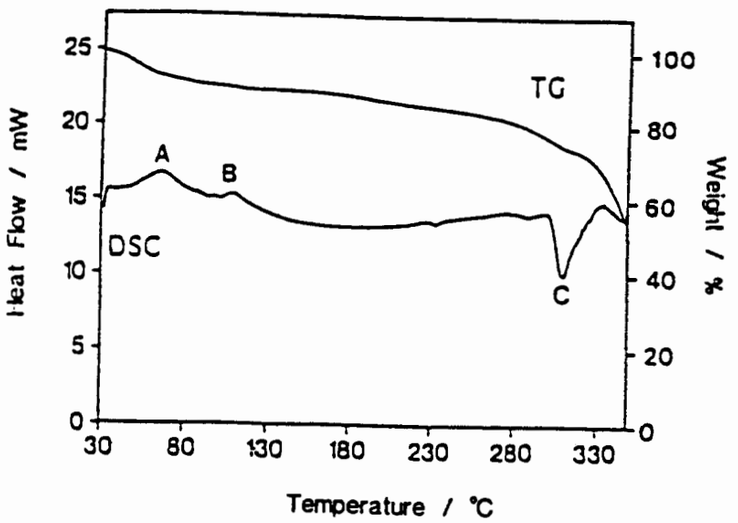

Figure 3.1 TG-DSC Traces for the complex COBCD

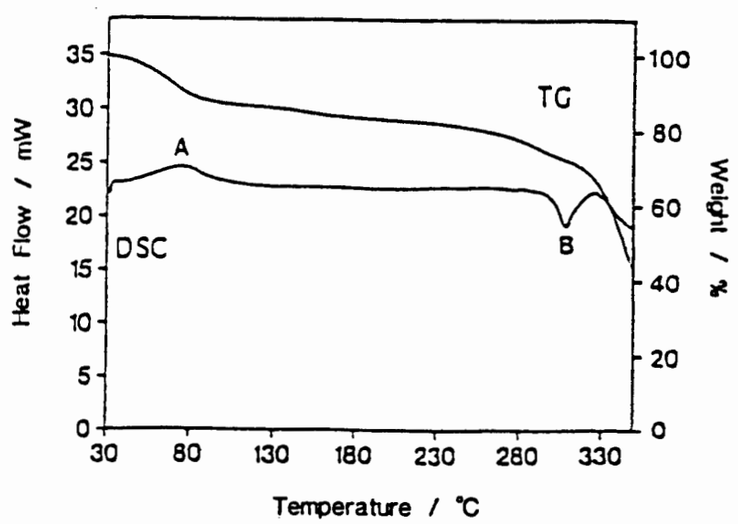

Figure 3.2 TG-DSC Traces for the complex COGCD

3.4 STOICHIOMETRY OF THE COMPLEXES

The stoichiometries of the complexes were determined by UV spectrophotometry and TG analysis. The chemical formulae for the complexes are shown in Tables 3.3 and 3.8. Both the COBCD and COGCD complexes contain 1:1 stoichiometric amounts of host and guest with 8.4 and 15.5 H_2O molecules per CD molecule respectively.

3.5 INFRARED SPECTROSCOPY (IR)

Since clofibric acid is a carboxylic acid, it was decided to assess the effect of complex formation on the carbonyl stretching frequency of clofibric acid. The carbonyl stretching frequency of pure clofibric acid was measured and found to occur at 1706 cm^{-1}. The carbonyl stretching frequency of the complexed drug in COBCD is displaced to 1730 cm^{-1}, and in COGCD to 1729 cm^{-1}. It is evident that the ν(C=O) of the complexed drug is significantly higher than in pure clofibric acid which suggests that the C=O bond is stronger in the complexed drug than in the uncomplexed acid. These shifts are similar to those observed by Wei et al.[5] from the IR spectra of tolbutamide complexes with permethyl-β-CD.

3.6 X-RAY POWDER DIFFRACTION

The complexes were characterised by XRD as described in section 2.6. This technique is very useful in helping to distinguish complexes from their respective physical mixtures. This is clearly illustrated in the XRD traces of COBCD, COGCD and their corresponding physical mixture of the respective CD with clofibric acid in Figure 3.3. In each case, the XRD pattern of the complex differs from that of the physical mixture allowing one to conclude that the complex represents a new crystalline phase.

A careful analysis of the XRD trace for COGCD reveals that the XRD pattern is relatively 'simple' in that it has few peaks. This is characteristic of compounds belonging to highly symmetrical space groups. All the crystallographic information is given in section 3.6.

(a)

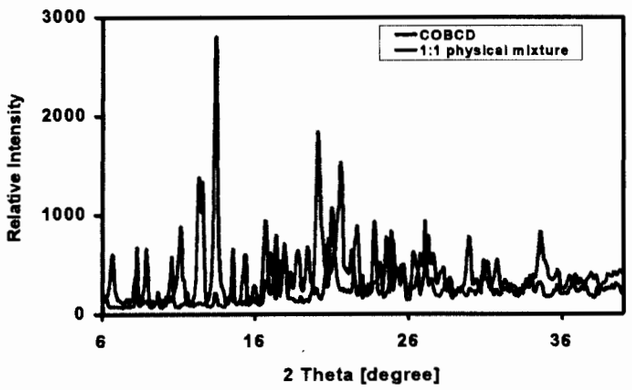

(b)

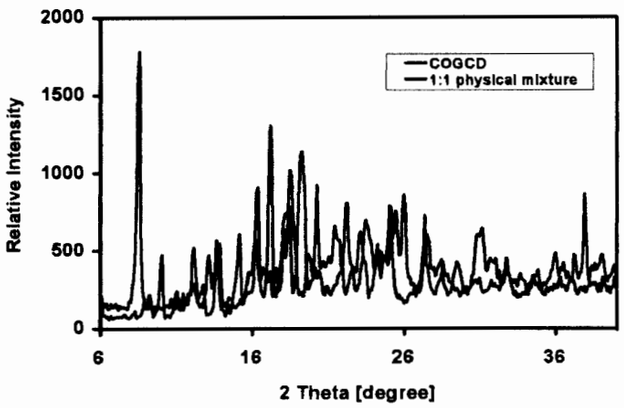

Figure 3.3 The XRD traces of (a) COBCD and 1:1 mixture of clofibric acid and β-CD (b) COGCD and 1:1 mixture of clofibric acid and γ-CD

3.7 CRYSTAL STRUCTURE ANALYSIS

3.7.1 DATA-COLLECTION

X-ray diffraction data for both COBCD and COGCD were collected on a Nonius Kappa CCD diffractometer using graphite-monochromated MoKα radiation at 293 K. A crystal of COBCD with dimensions 0.2 x 0.3 x 0.3mm was mounted on a glass fibre. The crystal was then covered in a cyanoacrylate adhesive to prevent cracking due to loss of water of crystallisation. A COGCD crystal of dimensions 0.3 x 0.4 x 0.3mm was treated in the same way. The detector to crystal distances were 50mm for both data-collections. A scan of 1.0° per image in ϕ was used in the range –120 to 120° for COBCD and –160 to 142° for COGCD.

3.7.2 COBCD COMPLEX

3.7.2.1 STRUCTURE DETERMINATION AND REFINEMENT

The crystal structure of COBCD was solved by the isomorphous replacement method using co-ordinates of the non-hydrogen atoms (excluding primary oxygen atoms, O(6)) of the host CD in the isomorphous β-CD complex of ibuprofen.[6]

The structure was refined by full-matrix least-squares refinement using the SHELXL-93 program[7] with subsequent location of remaining non-hydrogen atoms from the electron density map. The atoms O(6G1), O(6G2), O(6G4), O(6G5) and O(6G6) were found to be disordered, which means that each of them occupies at least two different sites. The site occupancy factors of the O(6) atoms are shown in Table 3.2.

All oxygen atoms except the disordered O(6) atoms were refined anisotropically with full site occupancy factor. Hydrogen atoms bonded to the carbon atoms of the host

were inserted in idealised positions (C-H distance of 0.98Å) and their common assigned temperature factor was allowed to refine freely, converging to $U_{iso} = 0.07Å^2$. Some electron density peaks (≤ 1.05 $eÅ^{-3}$) were observed in the difference Fourier map corresponding to the guest molecule in the β-CD cavity. These peaks could not, however, be interpreted as a meaningful representation of the guest drug molecule due to crystallographic disorder.

The structure refinement accounted for 7.0 H_2O molecules per CD molecule out of 8.4 H_2O estimated from TG analysis. Since the guest molecule could not be resolved, the refinement converged to a relatively high R_1-value of 0.12 for $I>2\sigma(I)$. The maximum and minimum residual electron densities were 1.05 and -0.52 $eÅ^{-3}$ respectively. Final fractional co-ordinates for all atoms of the host and water molecules in the COBCD complex are given in Appendix A on the appended diskette in ASCII format under the filename COBCD.TEX. Appendix B, also on diskette gives a full listing of observed (F_o) and calculated (F_c) structure factors. These are given under the filename COBCD.SFT.

Table 3.2 Site occupancy factors of the disordered O(6) atoms

Atom	Site Occupancy	
	A	B
O(6G1)	0.73	0.27
O(6G2)	0.62	0.39
O(6G4)	0.86	0.14
O(6G5)	0.69	0.31
O(6G6)	0.53	0.47

Table 3.3: Data-collection and refinement details for COBCD

Molecular formula	$C_{42}H_{70}O_{35}\cdot C_{10}H_{11}O_3Cl\cdot 8.4H_2O$
M_r/gmol^{-1}	1501
Crystal system	Monoclinic
Space group	C2
Z	4
a (Å)	18.82(1)
b (Å)	24.48(1)
c (Å)	15.76(1)
β (°)	110.43(1)
V (Å^3)	6802.6(5)
D_c (gcm^{-3})	1.465
Crystal dimensions (mm)	0.2x0.3x0.3
T/K	293
F(000)	3192
Initial settings	
θ (°)	4.3
κ (°)	0
ω (°)	180
Detector to crystal distance (mm)	50
Number of frames via ϕ	240
Δϕ scans (°) per frame	1
Exposure time (s)	160
Range scanned θ (°)	2.8≤θ≤26.4
Index range	h:0,23; k:-30,30; l:-19,17
Reflections collected	12828
Unique reflections	12631
Reflections with I>2σ(I)	9347
L.S. Parameters	546
R_1 (I>2σ(I))	0.1206
wR_2	0.3211
S	1.033
$(\Delta\rho)_{max}$ final (eÅ^{-3})	1.05
$(\Delta\rho)_{min}$ final (e Å^{-3})	-0.52

3.7.2.2 HOST-GUEST INTERACTION AND CRYSTAL PACKING

The numbering scheme for β-CD is shown in Figure 3.4 and that of the glucose moiety is shown in Figure 1.1(b). β-CD molecules in COBCD crystallise as head-to-head dimers through the formation of intermolecular hydrogen bonds between the O(3) atoms as shown in Figure 3.5. The intermolecular (intradimer) bonding distances are listed in Table 3.4. The dimers are stacked on top of each other along the *c*-axis yielding a channel-like structure. Figure 3.6 shows the channel packing of β-CD in the COBCD complex.

Table 3.4 Intermolecular hydrogen bonds between two β-CD molecules which form a dimer

Glucose Unit	$O(3G_n)\cdots O(3G_{8-n})$ distance (Å)
G1	2.86(1)
G2	2.87(1)
G3	2.78(1)
G4	2.92(1)
G5	2.78(1)
G6	2.87(1)
G7	2.87(1)

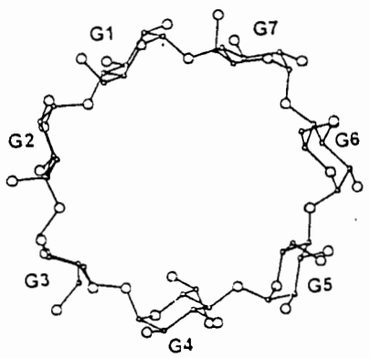

Figure 3.4 The β-CD molecule with its numbering scheme

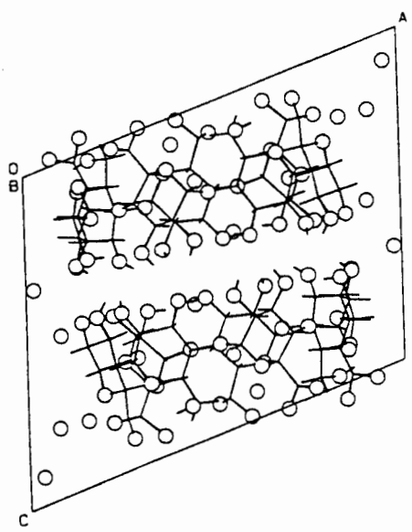

Figure 3.5 A view down [010] of the β-CD dimer. Oxygen atoms of the host and those of the water molecules are shown as open circles

The guest drug molecule is located inside the cavity, but it is disordered and could not be modelled to give a meaningful chemical structure. The electron density peaks located in the cavity, having a maximum value of about 1.05 $eÅ^{-3}$ reveal the approximate position of the guest molecule.

The disposition of these electron density peaks is shown in Fig 3.7. The disorder of the guest molecule is attributed to the highly diffusive state of the guest within the channel. Such disorder has been observed in other β-CD complexes which pack in a similar mode.[6,8-10] The water molecules of crystallisation form a hydrogen bonding network which facilitates the formation of infinite planes by the dimers as shown in the stereodrawing in Figure 3.8. Table 3.5 lists the hydrogen bonds between the water molecules and the hydroxyl groups of the host.

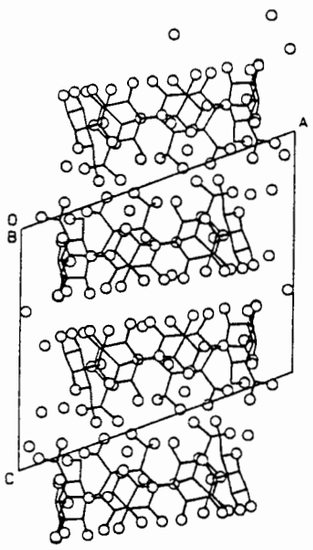

Figure 3.6 The channel packing mode of β-CD molecules in COBCD. Oxygen atoms of the host and those of the water molecules are shown as open circles

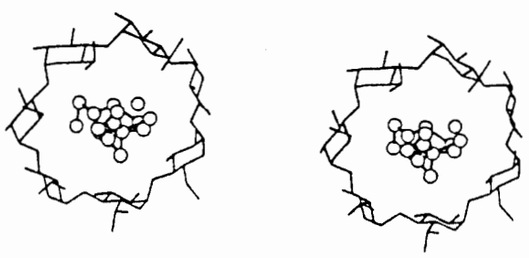

Figure 3.7 A Stereoview of the largest electron density peaks representing the guest molecule

Table 3.5: Hydrogen bonds between the hydroxyl groups of the host and H_2O molecules

O···O	Symmetry code for the second atom	Distance (Å)
O2G1···OW4	1/2-x, 1/2-y, 1-z	2.63(1)
O5G2···OW2	1/2-x, 1/2+y, -z	2.91(2)
O6G2···OW6	1/2-x, 1/2+y, -z	2.80(1)
O3G3···OW1	-x, y, 1-z	2.89(1)
O3G4···OW3	1-x, y, 1-z	2.81(1)
O3G5···OW4	1-x, y, 1-z	2.78(1)
O6G5···OW5	1-x, y, 1-z	2.79(3)
O3G6···OW3	1/2+x, 1/2+y, z	2.95(2)
O6G6···OW2	1/2+x, 1/2+y, z	2.75(2)
O6G6···OW6	1/2+x, 1/2+y, z	2.93(3)
O6G7···OW1	1/2-x, 1/2-y, 1-z	2.75(1)

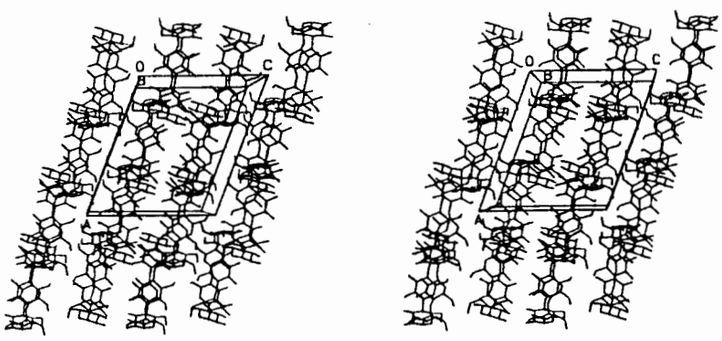

Figure 3.8: The infinite planes formed by β-CD molecules

3.7.2.3 CONFORMATION OF THE HOST MOLECULE

All seven α-D-glucose sub-units of the β-CD molecule exhibit a $^4C_1$ chair conformation. The primary hydroxyl group of the G(4) glucose unit is in a (–)-*gauche* conformation while the rest are in a (+)-*gauche* conformation. Geometric data such as radii of the O(4) heptagon, tilt angle, glycosidic angle, the O(4)···O(4) distances and the deviation of the O(4) atoms from their least-squares plane are given in Table 3.6. The tilt angles listed in Table 3.6 are all positive which means that the primary side of all seven glucose units leans toward the centre of the cavity. As a result, the β-CD molecule adopts a cone-like structure with the secondary side wider than the primary side. The conformation of the β-CD macrocycle is maintained by intramolecular $O(3G_n)\cdots O(2G_{n+1})$ bonds. This is similar to the situation in other β-CD complexes reported in literature.[6,11-13] The $O(3G_n)\cdots O(2G_{n+1})$ hydrogen bond distances are listed in Table 3.7.

Table 3.6: Geometric data for the β-CD molecule in COBCD

The glycosidic oxygen angle $C4G_n$-$O4G_n$-$C1G_{n+1}$ (°) and the torsion angle index (°)

C(4G1)-O(4G1)-C(1G2)	118.9(5)	G1	113.5
C(4G2)-O(4G2)-C(1G3)	119.5(4)	G2	125.5
C(4G3)-O(4G3)-C(1G4)	117.9(4)	G3	119.2
C(4G4)-O(4G4)-C(1G5)	118.6(4)	G4	121.1
C(4G5)-O(4G5)-C(1G6)	118.3(5)	G5	124.2
C(4G6)-O(4G6)-C(1G7)	119.0(4)	G6	123.5
C(4G7)-O(4G7)-C(1G1)	118.9(5)	G7	120.7

Glucose Unit	Tilt angle (°)	Radius of heptagon (Å)	$O(4G_n)...O(4G_{n+1})$ (Å)	Deviation (Å)
G1	2.6(3)	5.06(1)	4.34(1)	0.060(5)
G2	8.0(2)	5.22(1)	4.40(1)	-0.042(5)
G3	6.5(3)	5.02(1)	4.40(1)	-0.043(5)
G4	1.6(2)	4.97(1)	4.42(1)	0.069(5)
G5	4.1(2)	5.08(1)	4.32(1)	-0.002(5)
G6	7.2(2)	5.11(1)	4.37(1)	-0.086(5)
G7	0.6(2)	4.94(1)	4.47(1)	0.040(5)

All parameters in table are defined in section 1.5.2.1

Table 3.7: Intramolecular hydrogen bonds for the β-CD molecule

Glucose unit	$O(3G_n)\cdots O(2G_{n+1})$ (Å)
G1	2.85(1)
G2	2.91(1)
G3	2.83(1)
G4	2.77(1)
G5	2.80(1)
G6	2.80(1)
G7	2.75(1)

3.7.3 COGCD COMPLEX

3.7.3.1 STRUCTURE DETERMINATION AND REFINEMENT

The structure of COGCD was solved using co-ordinates for the non-hydrogen atoms (excluding the O(6) atoms) of the γ-cyclodextrin molecule in the isomorphous γ-CD·12-crown-4·LiSN complex.[12] The refinement was carried out using the SHELXL-93 program.[7] The missing atoms of the host as well as the H_2O molecules were located from subsequent electron density maps. Some of the oxygen atoms of the host CD were found to be disordered over two sites each. All non-hydrogen atoms were assigned anisotropic temperature factors. The refinement of this structure proved to be unsuccessful since the guest molecule could not be modelled beyond the diffuse electron density peaks in the CD cavity. Thermogravimetric analysis of the complex gave a weight loss which corresponded to 15.5 water molecules per CD molecule but only 6.3 H_2O molecules (which mainly occupy interstitial sites) were accounted for in the refinement. The data-collection and refinement details for COGCD are listed in Table 3.8. Final fractional co-ordinates for all atoms of the complex are given in

Appendix A on the appended diskette in ASCII format under the filename COGCD.TEX. Appendix B is also on diskette and is a full listing of observed (F_o) and calculated (F_c) structure factors. These are given under the filename COGCD.SFT.

3.7.3.2 HOST-GUEST INTERACTION AND CRYSTAL PACKING

In the COGCD crystal structure, three γ-CD molecules are stacked together in head-to-head, tail-to-tail and head-to-tail packing modes along the *c*-axis forming a channel-type structure. Figure 3.9 shows the three γ-CD molecules stacked together. In each γ-CD molecule, A, B and C, two glucopyranose residues form an asymmetric unit, from which the complete molecule is generated by the four-fold rotation axis. The glucose units are numbered as G1, G2 for molecule A, G3, G4 for molecule B and G5, G6 for molecule C. The atoms are numbered as A(nm) where A represents the atomic symbol, n is based on the numbering scheme for the glucose moiety as shown in Figure 1.1(b) (Chapter 1), and m is the number of the glucose moiety. The host and guest are centred on a four-fold rotation axis in a similar way to that shown in Figure 1.8. Molecules A and C have the same orientation and molecule B has the opposite orientation. Several intermolecular hydrogen bonds are formed between the secondary hydroxyl groups of A and B, the primary hydroxyl groups of B and C, and the primary hydroxyl groups A and the secondary hydroxyl groups of molecule C. This gives an endless channel-like structure, which accommodates clofibric acid and some water molecules. The guest molecule could not be resolved to reveal the exact mode of complexation due to crystallographic disorder exacerbated by the requirement of the four-fold symmetry of the contents of the cavity. The interstitial sites also assume a channel-like shape and are filled with water molecules as shown in Figure 3.10.

Table 3.8 Data-collection and refinement details for COGCD

Molecular formula	$C_{48}H_{80}O_{40}\cdot C_{10}H_{11}O_3Cl\cdot 15.5H_2O$
M_r/gmol^{-1}	1791
Crystal system	Tetragonal
Space group	$P42_12$
Z	6
a (Å)	23.65(1)
b (Å)	23.65(1)
c (Å)	23.64(1)
V (Å^3)	12896(8)
D_c (gcm^{-3})	1.383
Crystal dimensions (mm)	0.3x0.4x0.3
T/K	293
F(000)	5730
Initial settings	
θ (°)	8.5
κ (°)	180
ω (°)	0
Detector to crystal distance (mm)	50
Number of frames via ϕ	300
Δϕ scans (°) per image	1
Exposure time (s)	183
Range scanned θ (°)	2.5≤θ≤24.7
Index range	h:0,27; k:-19,19; l:0,26
Reflections collected	11207
Unique reflections	10960
Reflections with I>2σ(I)	6590
L.S.Parameters	634
R_1 (I>2σ(I))	0.1010
wR_2	0.2826
S	1.001
$(\Delta\rho)_{max}$final (eÅ^{-3})	0.64
$(\Delta\rho)_{min}$ final (e Å^{-3})	-0.58

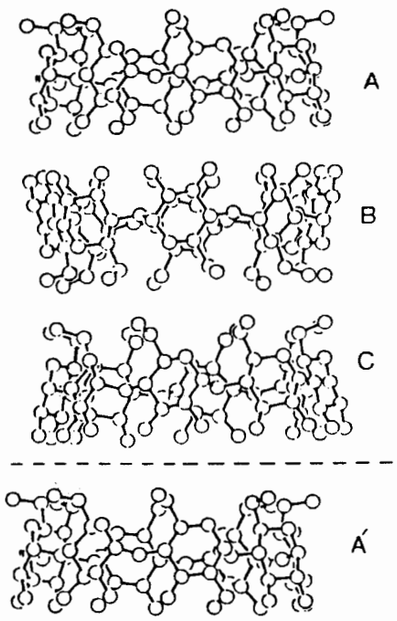

Figure 3.9 Channel structure of γ-CD in COGCD complex

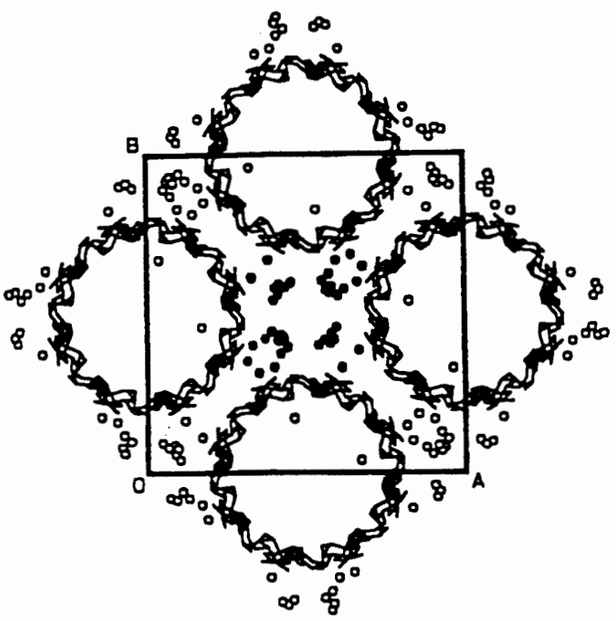

Figure 3.10 Crystal packing of the COGCD complex viewed down [010] with interstitial sites occupied by water molecules

3.7.3.3 CONFORMATION OF HOST MOLECULE

All glucose units of the three different γ-CD molecules are in the $^4C_1$ chair conformation. Table 3.9 list all important geometric parameters which describe the conformation of the macrocycle. The inter-glucose (glycosidic) bond angles range from 115.0(4) to 116.7(4)°. The distances of the O(4) atoms from the centre of gravity of the γ-CD macrocycle are in the range 5.82 to 5.90Å . This is defined as the radius of the octagon for γ-CD. The tilt angles range from 3.9-17.2°. The positive signs of these tilt angles indicate that the glucose moieties of all three γ-CD molecules are inclined with their primary side slightly turned toward the centre of the macrocycle. The round shape of the macrocycle is maintained by the formation of intramolecular hydrogen bonds between the secondary hydroxyl groups reflected in the O(2)···O(3) distances between the neighbouring glucose residues. The intramolecular hydrogen bond distances are listed in Table 3.10.

Table 3.9: Geometric parameters for the γ-CD molecules in COGCD

The glycosidic oxygen angle $C4G_n$-$O4G_n$-$C1G_{n+1}$ (°) and the torsion angle index (°)

Glycosidic angle	(°)	M	G	(°)
C(41)-O(41)-C(12')	116.7(5)	A	G1	113.5
C(42)-O(42)-C(11)	116.7(4)		G2	125.5
C(43)-O(43)-C(14')	116.1(4)	B	G3	119.2
C(44)-O(44)-C(13)	116.1(4)		G4	121.1
C(45)-O(45)-C(16')	115.0(5)	C	G5	124.2
C(46)-O(46)-C(15)	115.0(4)		G6	123.5

M	G	Tiit angle (°)	Radius of heptagon (Å)	$O(4G_n)...O(4G_{n+1})$ (Å)	Deviation (Å)
A	G1	13.7(2)	5.88(1)	4.49(1)	-0.004(4)
	G2	3.9(1)	5.87(1)	4.50(1)	0.005(5)
B	G3	15.6(3)	5.85(1)	4.50(1)	-0.003(4)
	G4	13.3(2)	5.83(1)	4.50(1)	0.004(4)
C	G5	17.2(2)	5.90(1)	4.49(1)	-0.015(4)
	G6	5.8(2)	5.82(1)	4.49(1)	0.017(5)

All geometric parameters are defined in section 1.5.2.1, M = γ–CD molecule and G=Glucose unit

Table 3.10 The intramolecular hydrogen bonds between neighbouring glucose units

γ-CD Molecule	Glucose unit	O···O	H-Bond distances (Å)
A	G1	O(21)···O(32)	2.77(1)
	G2	O(22)···O(31')	2.82(1)
B	G3	O(23)···O(34)	2.84(1)
	G4	O(24)···O(33')	2.89(1)
C	G5	O(25)···O(36)	2.89(1)
	G6	O(26)···O(35')	2.87(1)

3.8 KINETICS OF DEHYDRATION

Water molecules play an essential role in stabilising the crystalline structure of cyclodextrin inclusion compounds. Complex water content as well as the nature and the rate of dehydration affect properties such as cohesive strength and stability under storage. The kinetics of dehydration of the two complexes (COBCD and COGCD) and their respective host compounds were investigated by isothermal thermogravimetry. It was of particular interest to compare the activation energies of dehydration of the complexes with those for the uncomplexed hydrated parent CDs. In this section we report the results of the kinetics of dehydration in relation to crystal structure.

3.8.1 RESULTS FOR THE KINETICS OF DEHYDRATION

The kinetics of dehydration studies were carried out over the temperature range of 35-70 °C. The α-time curves for COBCD and COGCD are best described by the D3 (three dimensional diffusion-controlled) model, whereas those of β-CD and γ-CD hydrates are best described by the F1 (first order) and F2 (second order) kinetic models respectively. Figure 3.11 shows a representative α-time curve for COBCD at 55 °C. The Arrhenius (ln k vs. 1/T) plots for the compounds studied were linear over the investigated temperature range as shown in Figure 3.12. Kinetic data for the dehydration of COBCD, COGCD, β-CD·12.5H_2O and γ-CD·16.8H_2O are listed in Table 3.11. The activation energies for the dehydration of the complexes are significantly lower than those of their corresponding parent hydrated CDs. It should be noted that the activation energy (E_a) obtained here for the dehydration of β-CD·12.5H_2O, 64 ± 2 kJ mol^{-1}, compares favourably with the value 65.7 ± 3.1 kJ mol^{-1} obtained earlier,[14] although the non-isothermal methods used led to the conclusion that the dehydration is a zero-order process. On the other hand, first-order dehydration kinetics were reported for the hydrated β-CD from the analysis of diffraction data measured from a single crystal exposed to a range of relative humidities.[15] In any event the use of 64 ± 2 kJ mol^{-1} for the dehydration of β-CD hydrate obtained in this study seems to be justified in view of the insensitivity of derived E_a values to the reaction order and the fact that it is being compared to the E_a values for other compounds obtained under the same conditions.

Table 3.11 Kinetic parameters for dehydration of complexes COBCD and COGCD and their corresponding uncomplexed parent CD hydrates.

Species	Kinetic model for dehydration	E_a / kJ mol^{-1}	Regression coeff. Arrhenius plot
COBCD	D3	50 ± 2	0.9911
COGCD	D3	43 ± 1	0.9973
β-CD·12.5H_2O	F1	64 ± 2	0.9978
γ-CD·16.8H_2O	F2	58 ± 4	0.9951

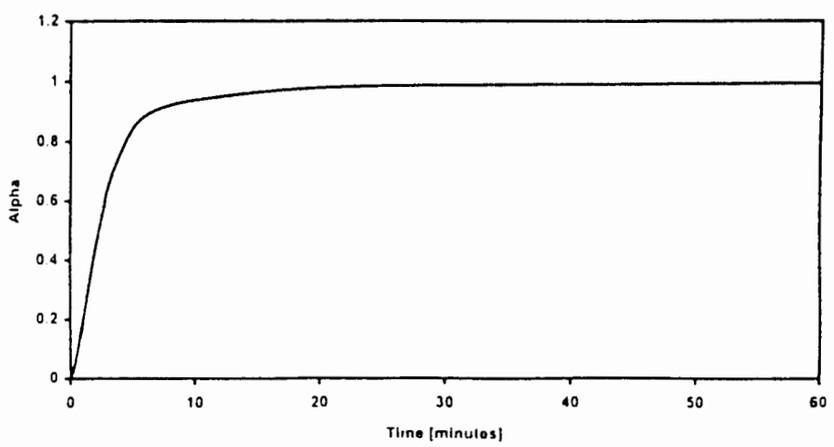

Figure 3.11 The α vs. time curve for the complex COBCD at 55 °C

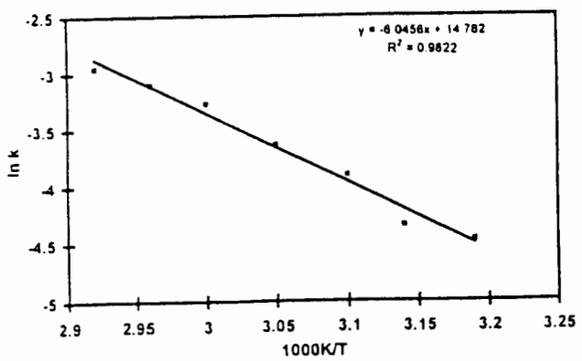

(a)

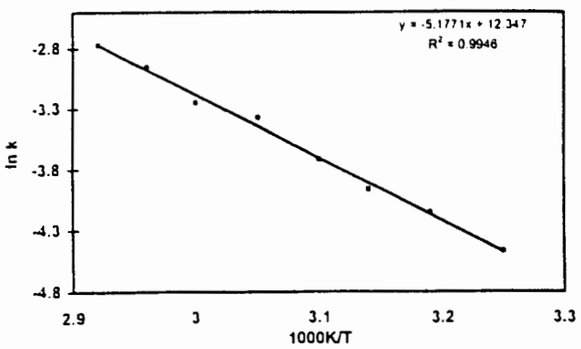

(b)

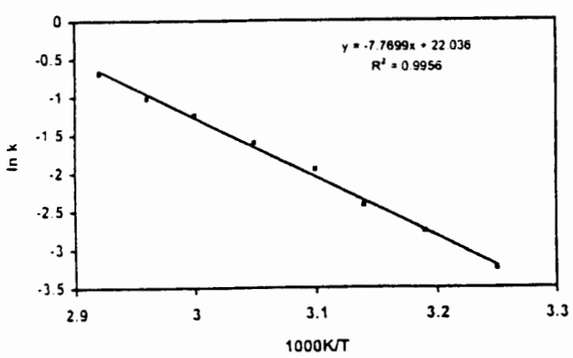

(c)

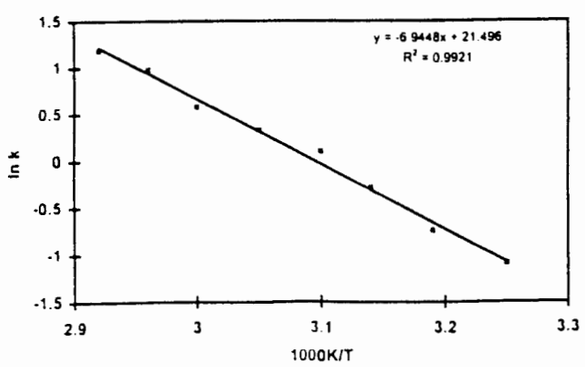

(d)

Figure 3.12: Arrhenius plots for (a) COBCD, (b) COGCD , (c) β-CD hydrate and (d) γ-CD hydrate

3.8.2 KINETICS OF DEHYDRATIONS IN RELATION TO CRYSTAL STRUCTURE

As described in 3.7.2.2 and 3.7.3.2, both COBCD and COGCD complexes pack in channel mode and the channels are occupied by water molecules as shown in Figures 3.13 and 3.10 respectively. The program MOLMAP[16] was used to examine the water-filled channel topologies. The program MOLMAP reads a SHELX-93 input file and allows one to plot slices through the unit cell at constant intervals. Atoms of the water molecules were removed from the input file, leaving the host atoms which were assigned their van der Waals radii. This revealed the continuity and unconstrained nature of the channels along the *z*-direction in the crystals. The channel cross-sectional areas vary between 34-57 $Å^2$ in COBCD and 44-97 $Å^2$ in COGCD. Thus, migration of H_2O molecules along these channels should be unimpeded by the host CD molecules in both complexes. These results are consistent with the finding that the dehydration of both COBCD and COGCD follow a diffusion-controlled kinetic model. A detailed study of the packing in the β-CD hydrate structure[15] showed that there are no diffusion paths for H_2O molecules in the static structure and that dehydration must involve some conformational flexure of the host molecule to create such pathways. This crystal structure and that of γ-CD hydrate are of a 'cage' type[17] with water molecules 'locked' in the interstitial cavities and within the CD cavities. It is therefore reasonable to conclude that the lower activation energy obtained for the dehydration of complexes COBCD and COGCD as compared to their parent CD hydrates are consistent with the location of the water molecules in unobstructed channels, which could facilitate water escape from the crystal. β-CD and γ-CD complexes frequently crystallise in the respective space groups C2 and $P42_12$ and we predict, on the basis of their isomorphism with COBCD and COGCD, that their

dehydration will also be characterised by relatively low activation energies.

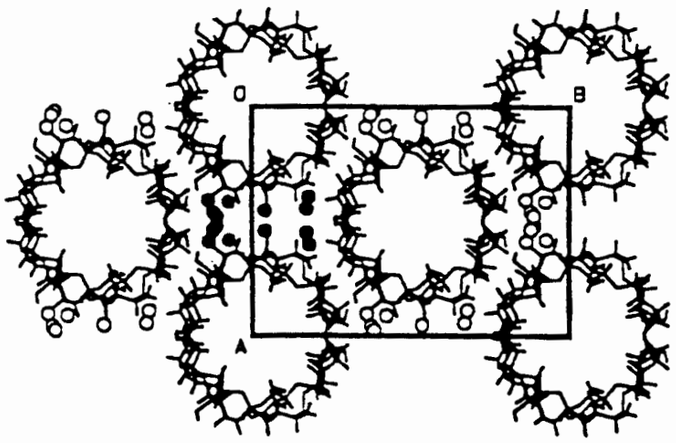

Figure 3.13 Projection of the crystal structure of COBCD parallel to the host channel, showing interstitial water molecules

3.9 REFERENCES

1. S. Anguiano-Igea, F. J. Otero-Espinar, J. L. Vila-Jato and J. Blanco-Méndez, *Int. J. Pharm.,* 1996, **135,** 161.
2. Z. Aigner, I. Bencz and M. Kata, *J. Incl. Phenom.*, 1994, **20**, 241.
3. W. C. Bowman and M. J. Rand, Text Book of Pharmacology, 2nd Ed, Blackwell Scientific Publication, Oxford, 1980.
4. C. H. L Kennard, G. Smith and A. H. White, *Acta Cryst.*, 1982, **B38**, 868.
5. Y. C. Wei, A. M. Knevel, G. P. Carlson and C. J. Chang, *J. Incl. Phenom.*, 1996, **25**, 69.
6. G. R. Brown, *Physicochemical Characterisation of Cyclodextrin Inclusion Compounds with Non-steroidal Anti-inflammatory Drugs,* MSc Thesis, University of Cape Town, 1997.
7. G. M. Sheldrick, SHELXL-93, *Program for the Refinement of Crystal Structures,* University of Göttingen, Germany, 1993.
8. I. M. Mavridis and E. Hadjoudis; *Carbohydrate Res.,* 1991, **11**, 220.
9. G. Le Bas, C. De Rango, N. Rysanek and G. Tsoucaris, *J. Incl. Phenom.*, 1984, **2**, 861.
10. C. Betzel, B. Hingerty, N. Noltemeyer, G. Weber, W. Saenger and J. A. Hamilton, *J. Incl. Phenom.*, 1983, **1**, 1181.
11. S. Kamitori, K. Hirotsu and K. Higuchi, *J. Am. Chem. Soc.*, 1987, **109**, 2409.
12. C. Betzel, B. Hingerty, W. Saenger and G. M. Brown, *J. Am. Chem. Soc.*, 1984, **106**, 7545.
13. M. R. Caira, V. J. Griffith, L. R. Nassimbeni and B. van Oudtshoorn, *J. Incl. Phenom.*, 1994, **17**, 187.

14. A. Szafranek, *J. Thermal. Anal.,* 1988, **34**, 917.

15. T. Steiner and G. Koellner, *J. Am. Chem. Soc.*, 1994, **116**, 5122.

16. L. J. Barbour, *Clathration by Diol Hosts*: *Thermodynamics and Structure*, PhD Thesis, University of Cape Town, 1994.

17. K. Harata, *Bull. Chem. Soc. Jpn.*, 1987, **60**, 2763.

CHAPTER FOUR

CHAPTER 4: DIMEB AND TRIMEB COMPLEXES OF CLOFIBRIC ACID

4.1 INTRODUCTION

The significantly greater solubility of methylated β-CDs as compared to their parent CDs makes them ideal for pharmaceutical application. These molecules are also known to have higher complexing ability than their corresponding native CDs. Since the guest molecules in COGCD and COBCD are disordered, as reported in Chapter 3, it was decided to consider studying inclusion complexes of clofibric acid with methylated CDs which are generally known to yield ordered structures. The complexes were prepared as reported in section 2.4. In this chapter we report data for the solid complexes of Dimeb and Trimeb with clofibric acid, which are determined mainly by thermal analysis as well as X-ray structure analysis. The Dimeb and Trimeb complexes of clofibric acid will be referred to as CODMB and COTMB respectively.

4.2 THERMAL ANALYSIS

The DSC-TG traces of CODMB and COTMB are shown in Figures 4.1 and 4.2, and the data are listed in Table 4.1. The dehydration of both complexes is endothermic (Endo A). The anhydrous CODMB complex undergoes a phase transition at 151.4 °C (Endo B) followed by decomposition at 206 °C (Endo C).

The dehydration process of COTMB occurred over a wide temperature range despite the fact that COTMB contains only about 1.5% H_2O by mass as determined by TG.

Other interesting features were observed on the DSC traces of COTMB; the anhydrous COTMB complex undergoes an endothermic phase change (endo B), recrystallization, and finally melting which is represented by peak C. The proposed phase transition is consistent with zero mass loss (from TG) over the temperature range which includes peaks B and C. To confirm the nature of the phase transition, X-ray diffractograms were recorded for COTMB samples that had been heated to approximately 100, 135 and 200 °C then allowed to cool to ambient temperature. The first two samples yielded different X-ray powder patterns, thus confirming the existence of two distinct crystalline phases, while the last yielded a diffuse pattern only, indicating that the final residue was essentially amorphous.

Table 4.1 DSC-TG data for CODMB and COTMB

complex	Event (DSC)	Onset (T/ °C)	Peak (T/ °C)	% H_2O (TG)	H_2O molecules per CD molecule
CODMB	Endo A	54.1	76	5.9	5.4
	Endo B	148.9	151.4		
	Endo C	201	206.5		
COTMB	Endo A	30	45	1.5	1.4
	Endo B	129	132		
	Endo C	145	147		

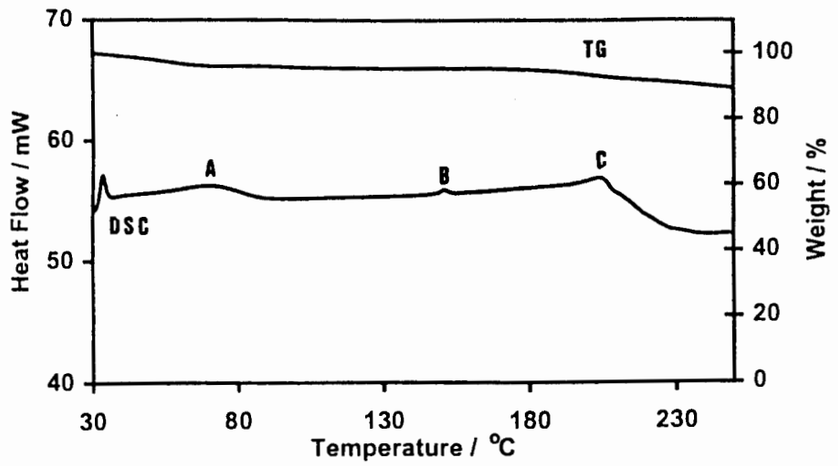

FIGURE 4.1: TG-DSC traces for the CODMB complex

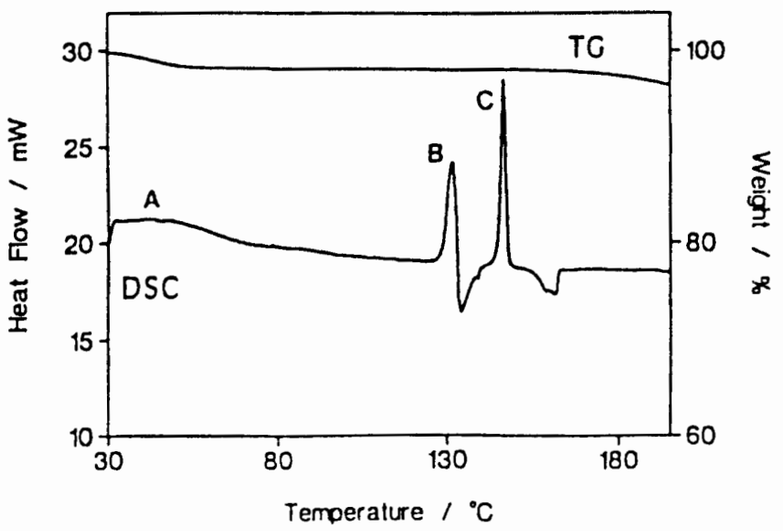

FIGURE 4.2 TG-DSC traces for the COTMB complex

4.3 STOICHIOMETRY OF COMPLEXES

The stoichiometries of the complexes were determined by using both TG and UV spectrophotometry. TG was used to determine the amount of water present in the complex while UV spectrophotometry was used to determine the drug content. Both complexes have 1:1 drug-CD molar ratio and their H_2O contents are 5.4 and 1.4 H_2O molecules per CD molecule for CODMB and COTMB respectively. The full chemical formulae for the complexes are listed in Tables 4.2 and 4.3.

4.4 INFRARED SPECTROSCOPY

Infrared spectroscopy was also used to study the complexes CODMB and COTMB. The C=O stretching frequencies of the complexed drugs in CODMB and COTMB are displaced to 1734 and 1726 cm^{-1} respectively from the value of 1706 cm^{-1} for the drug itself. These shifts are similar to the ones observed in the IR spectra of COBCD and COGCD (Chapter 3). The crystal structure solution for COTMB has helped to clarify what causes C=O stretching frequency shift (see section 4.5.5). The host-guest interaction as well as molecular packing in COTMB are discussed in detail in section 4.5.

4.5 X-RAY STRUCTURE ANALYSIS

4.5.1 DATA-COLLECTION

X-ray diffraction data for both CODMB AND COTMB were collected on a Nonius Kappa CCD diffractometer using graphite-monochromated MoKα radiation at 293 K. For CODMB a single crystal was mounted on a glass fibre. Since the complex has small water content, the crystal was stable and no special treatment was necessary. A crystal of COTMB was treated in the same way. Crystal data and data-collection strategies for the CODMB complex are listed in Table 4.2.

4.5.2 STRUCTURE DETERMINATION AND REFINEMENT

CODMB

The isomorphous replacement technique was inappropriate since no published coordinates were available for isomorphous structures. The strategy employed in attempting to solve the structure by direct methods involved using options available in the program SHELXS-86,[1] for example varying the starting reflection subsets, the value of E_{min} and the number of cycles of tangent refinement. Numerous computations were performed but none of these yielded a phase set with a combined figure of merit less than 0.18 and no E-map revealed a sensible molecular fragment. Several attempts to solve the structure by Patterson search methods using the program PATSEE[2] were also unsuccessful. Due to time constraints, it was necessary to abandon further attempts.

Table 4.2 Data-collection and cell data for CODMB

Molecular formula	$C_{56}H_{98}O_{35}\cdot C_{10}H_{11}O_3Cl\cdot 5.4H_2O$
M_r/gmol^{-1}	1643.3
Crystal system	Orthorhombic
Space group	$P2_12_12_1$
Z	4
a (Å)	10.78(1)
b (Å)	15.34(1)
c (Å)	49.39(1)
V (Å^3)	8167(4)
D_c (g cm^{-3})	1.336
Crystal dimensions (mm)	0.3x0.4x0.3
T/K	293(1)
F(000)	3520
Detector to crystal distance (mm)	50
Set 1	
Initial settings	4.7
θ (°)	0
κ (°)	180
ω (°)	
Number of frames via ϕ	320
Δϕ scans (°) per image	0.5
Exposure time (s)	243
Set 2	
Initial settings	
ϕ (°)	102.4
θ (°)	-9.8
κ (°)	-148
Number of frames via ω	85
Δω scans (°) per image	0.5
Exposure time (s)	243
Reflections collected	7492
Unique reflections	7477

COTMB

The crystal structure of COTMB was solved by the isomorphous replacement method using co-ordinates of non-hydrogen atoms (excluding O(6), C(7), C(8) and C(9) atoms) of the host Trimeb in the isomorphous Trimeb complex of menthol.[3] The structure was refined by full-matrix least-squares using the program SHELXL-93[4] with subsequent location of the remaining non-hydrogen atoms of the host, guest and the water molecules from successive electron density maps. Hydrogen atoms bonded to the carbon atoms of the both host and guest were inserted in idealised positions (C-H bond length of 0.98Å) and their separate common variable temperature factors were allowed to refine freely. Since TG analysis indicated 1.4 H_2O molecules per CD molecule, the water content was modelled based on these data. The 1.4 H_2O molecules appeared to be distributed over two sites, with site occupancy factors of 0.89 and 0.51. The structure solution appeared to be successful as the guest molecule was clearly resolved. The refinement converged to an R_1-factor of 0.087 based on observed reflections with $I>2\sigma(I)$. The maximum and minimum residual electron densities were 0.709 and -0.854 e $Å^{-3}$ respectively.

Table 4.3: Data-collection and refinement details for COTMB

Molecular formula	$C_{63}H_{112}O_{35}\cdot C_{10}H_{11}O_3Cl\cdot 1.4H_2O$
M_r/gmol^{-1}	1669.4
Crystal system	Orthorhombic
Space group	$P2_12_12_1$
Z	4
a (Å)	11.60(1)
b (Å)	26.28(1)
c (Å)	28.88(1)
V (Å^3)	8807(4)
D_c (gcm^{-3})	1.259
Crystal dimensions (mm)	0.2x0.3x0.3
T/K	293
F(000)	3584
Initial settings	
θ (°)	10
κ (°)	0
ω (°)	180
Detector to crystal distance (mm)	45
Number of frames via ϕ	360
Δϕ scans (°) per image	1
Exposure time (s)	142
Range scanned θ (°)	1.1≤θ≤28.3
Index range	h:0,15; k:-34,35; l:-38,38
Reflections collected	41775
Unique reflections	21770
Reflections with I>2σ(I)	6760
L.S. Parameters	758
R_1 (I>2σ(I))	0.0872
wR_2	0.2390
S	0.832
$(\Delta\rho)_{max}$final (eÅ^{-3})	0.71
$(\Delta\rho)_{min}$ final (e Å^{-3})	-0.85

4.5.3 MOLECULAR PACKING AND HOST-GUEST INTERACTION

The numbering schemes for clofibric acid and the glucose units of Trimeb are shown in Figure 4.3. The carboxylic oxygens were distinguished from each other based on the magnitudes of their bond lengths. O(13) represents the carbonyl oxygen atom while O(14) is a hydroxyl oxygen atom. The mode of drug inclusion is rather unusual in COTMB. The carboxylic group of the guest is buried inside the cavity, instead of the chlorophenyl ring, as one might have expected. The insertion occurs on the O(2), O(3) side of the Trimeb cavity as shown in Figure 4.4. The two oxygen atoms O(13) and O(14) of the carboxylic group of clofibric acid form hydrogen bonds with the water molecules O(W2) and O(W1) respectively. The O(W1) and (OW2) molecules in turn form hydrogen bonds with the disordered O(6G4) atoms of the host (see Figure 4.4). The intermolecular hydrogen bonds are listed in Table 4.4. The primary (O(6)) side is virtually closed up by the C(9) methyl groups giving the interior of the cavity a cup-shaped structure. Figure 4.5 shows space-filling diagrams which reveal how the guest molecule is buried in the cup-shaped Trimeb cavity. The chlorophenyl ring of the guest molecule makes a dihedral angle of 78.9(2)° with the O(4) plane of the host molecule. The hydrogen bonds between water molecules and the guest molecules play a role in stabilising the complex. Complex units for COTMB are packed in a head-to-tail fashion in a continuous channel mode along the *a*-axis as shown in Figure 4.6.

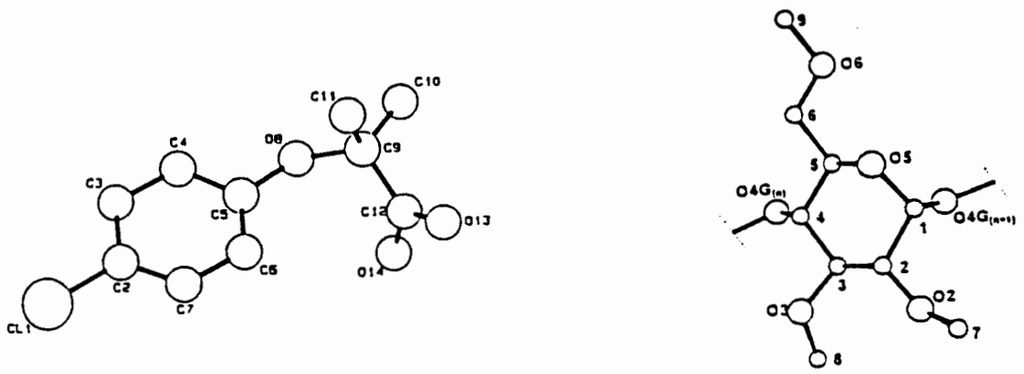

Figure 4.3 The numbering schemes for clofibric acid (left) and permethylated glucose unit (right)

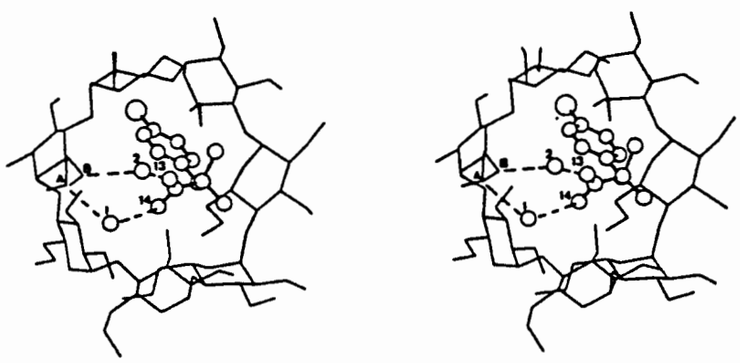

(a) View into the Trimeb cavity from the primary side

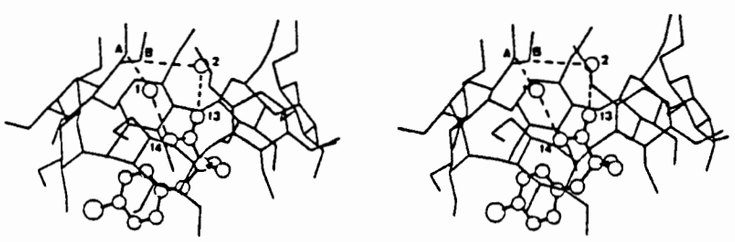

(b) View perpendicular to the host axis

Figure 4.4 Stereodiagrams of the COTMB complex

In the diagrams, A = O(6G4A) and B = (O6G4B), 1 and 2 represent the oxygen O(W1) and O(W2) atoms of the water molecules, 13 represent O(13), the cabonyl O atom and 14 represent O(14), the hydroxyl O atom (see Table 4.4).

(a)

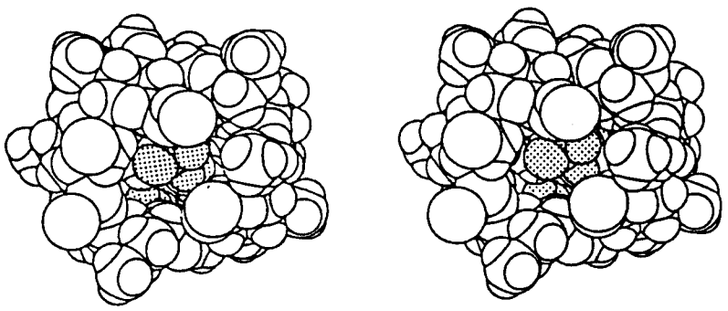

(b)

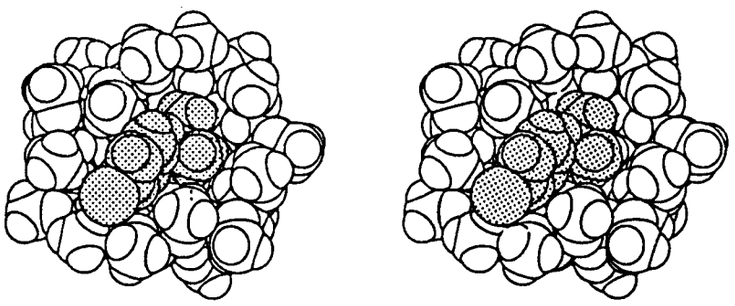

(c)

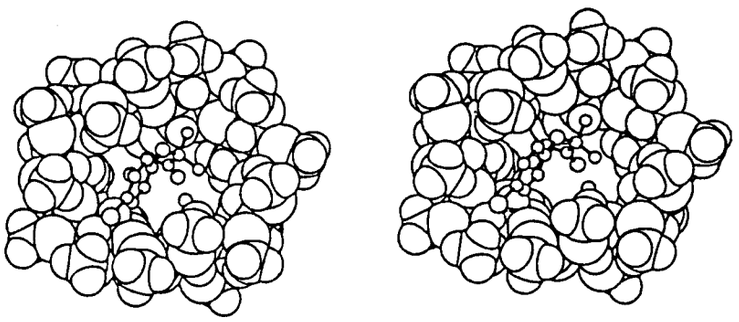

Figure 4.5 Space-filling diagrams of the COTMB complex (a) from the O(6) side of the host, (b) from the O(2),O(3) side of the host and (c) the stick representation of guest in (b)

Table 4.4: Intermolecular hydrogen bonds

O···O Contacts	Distance (Å)
O(13)···O(W2)	2.53(1)
O(14)···O(W1)	2.70(1)
O6G4(A)···O(W1)	2.76(1)
O6G4(B)···O(W2)	2.59(2)

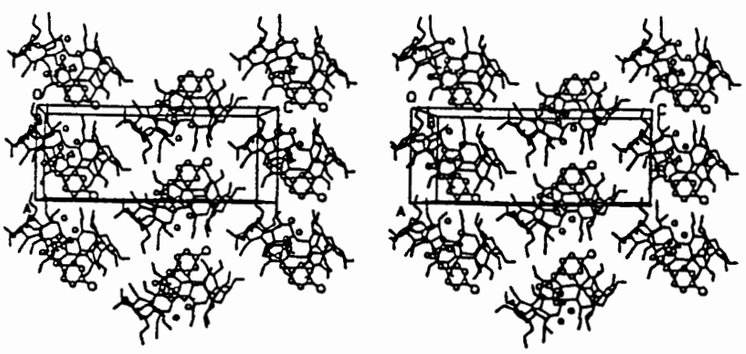

Figure 4.6 Packing diagram for COTMB viewed down the *b*-axis. For clarity, only three columns of the complex molecules are illustrated

4.5.4 HOST CONFORMATION

The conformation of the Trimeb molecule in COTMB is similar to that occurring in many complexes reported in the literature. All methylated glucose residues of the Trimeb molecule are in a $^4C_1$ chair conformation. Four of the C(9) atoms of the methyl glucose units show disorder, namely C(9G1), C(9G2), C(9G4), C(9G7). Generally, the bond lengths and bond angles conform to those of other known cyclodextrin complexes except

for the disordered atoms mentioned above. The C(6)-O(6) bonds in G4 and G5 have a (+)-*gauche* conformation, while all other C(6)-O(6) bonds are in a (-)-*gauche*[5] conformation. All important geometric parameters for the Trimeb molecule such as radii of the O(4) heptagon, tilt angles, glycosidic angles, O(4)···O(4') distances and the deviations of the O(4) atoms from their least-squares plane are listed in Table 4.5. From the tilt angles listed in Table 4.5, it is evident that the G1, G3, G4, G5 and G7 glucose units are tilted in such a way that O(6)-C(9) groups almost close up the primary side of the Trimeb molecule. The shape of the Trimeb molecule is maintained by six intramolecular C-H···O hydrogen bonds, namely the $C(6G_n)$-H···$O(5G_{n-1})$ bonds which are listed in Table 4.6.

4.5.5 GUEST CONFORMATION

Except for the orientation of the carboxylic group, the conformation of the clofibric acid molecule in the COTMB complex is similar to that occurring in pure clofibric acid as reported by Kennard et al.[6] Table 4.7 shows the interatomic distances and angles about the carboxylic chain for complexed and pure drug molecules while the relevant torsion angles are shown in Table 4.8. The numbering scheme used for clofibric acid is shown in Figure 4.3. A comparison of the C=O bond distances in the complexed and uncomplexed clofibric acid showed that the C=O length of the complexed drug is significantly shorter (1.17(1)Å) than in the uncomplexed drug (1.231(6)Å). These results are in good agreement with the IR data (section 4.4).

Table 4.5 Geometric data for the Trimeb molecule in COTMB

The glycosidic oxygen angle $C4G_n$-$O4G_n$-$C1G_{n+1}$ (°) and the torsion angle index (°)

C(4G1)-O(4G1)-C(1G2)	116.9(5)	G1	128.7
C(4G2)-O(4G2)-C(1G3)	118.3(5)	G2	135.8
C(4G3)-O(4G3)-C(1G4)	117.9(5)	G3	104.5
C(4G4)-O(4G4)-C(1G5)	114.8(5)	G4	136.7
C(4G5)-O(4G5)-C(1G6)	118.8(5)	G5	142.4
C(4G6)-O(4G6)-C(1G7)	117.4(4)	G6	113.5
C(4G7)-O(4G7)-C(1G1)	116.4(5)	G7	133.1

Glucose unit	Tilt angle (°)	Radius of heptagon (Å)	$O(4G_n)...O(4G_{n+1})$ (Å)	Deviation (Å)
G1	26.7(2)	5.13(1)	4.45(1)	-0.537(4)
G2	-12.9(2)	5.41(1)	4.34(1)	0.157(5)
G3	9.9(2)	4.94(1)	4.62(1)	0.388(4)
G4	47.3(2)	5.20(1)	4.31(1)	-0.216(4)
G5	20.5(2)	4.60(1)	4.23(1)	-0.489(5)
G6	-14.8(2)	5.13(1)	4.53(1)	0.457(4)
G7	42.4(2)	5.10(1)	4.28(1)	0.078(4)

All parameters are described in section 1.5.2.1

Table 4.6 Intramolecular C-H···O hydrogen bonds in COTMB

			Distance (Å)			Angle(°)
C	**H**	**O**	**C···O**	**C-H**	**H···O**	**C-H···O**
C(6G1)	H(6G1A)	O(5G7)	3.19(1)	0.97(1)	2.51(1)	138.1
C(6G2)	H(6G2A)	O(5G1)	3.37(1)	-	-	
C(6G3)	H(6G3A)	O(5G2)	3.16(1)	0.97(1)	2.55(1)	123.4
C(6G5)	H(6G5A)	O(5G4)	3.22(1)	-	-	
C(6G6)	H(6G6A)	O(5G5)	3.16(1)	0.97(1)	2.72(1)	127.6

(-) No hydrogen atoms were attached to the C(6G2) and C(6G5) atoms because they are disordered.

Table 4.7 Interatomic distances (Å) and angles (°) associated with the the carboxylic acid

	Complexed clofibric acid	Uncomplexed clofibric acid[6]
C(12)-O(13)	1.17(1)	1.231(6)
C(12)-O(14)	1.30(1)	1.283(6)
C(9)-C(12)-O(13)	123.4(1)	119.3(2)
C(9)-C(12)-O(14)	113.6(1)	111.6(4)
O(13)-C(12)-O(14)	123.0(1)	124.0(5)

Table 4.8: Selected torsion angles

	Complexed clofibric acid	Uncomplexed clofibric acid [6]
C(4)-C(5)-O(8)-C(9)	149.1(7)	130.4(2)
C(5)-O(8)-C(9)-C(12)	70.7(9)	79.0(2)
O(8)-C(9)-C(12)-O(14)	28.5(9)	-35.9(2)

The angles C(4)-C(5)-O(8) and C(6)-C(5)-O(8) whose values are 109.3(7)° and 128.4(7)° respectively show significant deviations from the expected trigonal angle of 120°. Similar deviations have also been observed in the crystal structure of pure clofibric acid where the corresponding angles were 114.2(2)° and 124.0(2)° respectively.[6] Such deviations are due to molecular crowding caused by the steric requirement of the bulky isopropionic acid side chain. The deviations are somewhat larger in the complexed drug than in pure clofibric acid. Such differences can be attributed to the fact that the isopropionic acid side chain is more nearly coplanar with the chlorophenyl ring in the complexed clofibric acid than in the uncomplexed clofibric acid.

4.6 X-RAY POWDER DIFFRACTION (XRD)

The complexes were characterised by XRD as described in Section 2.6. The calculated XRD pattern for the COTMB complex was obtained by using a program LAZYPULVERIX[7] on a personal computer running in the DOS operating system. The XRD patterns for the CODMB complex and the 1:1 physical mixture of clofibric acid with Dimeb are shown in Figure 4.7.

The XRD pattern for CODMB is distinctive and differs significantly from that of the 1:1 physical mixture. This confirms that CODMB is a new phase with its own characteristic crystal structure. The experimental and calculated XRD patterns for COTMB are shown in Figure 4.8. There are very close matches in the peak positions as well as in the relative intensities for the calculated and experimental XRD patterns. This demonstrates that the sample used for the experimental XRD analysis is of high purity.

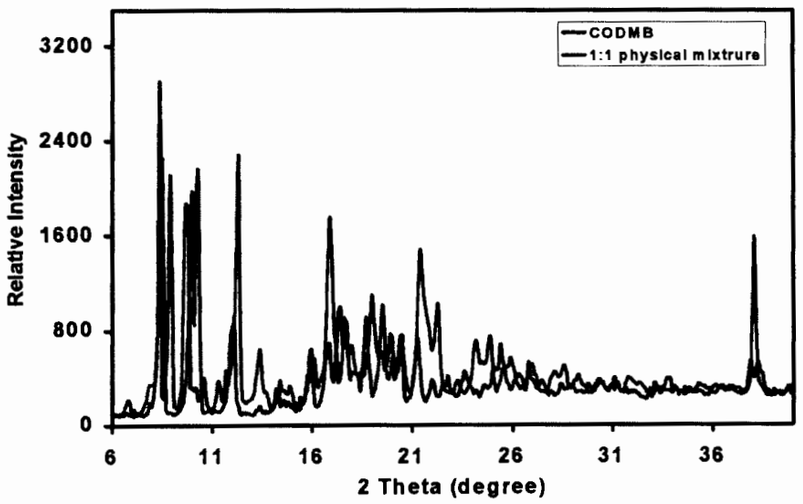

Figure 4.7 XRD traces of CODMB and 1:1 physical mixture of Dimeb with clofibric acid

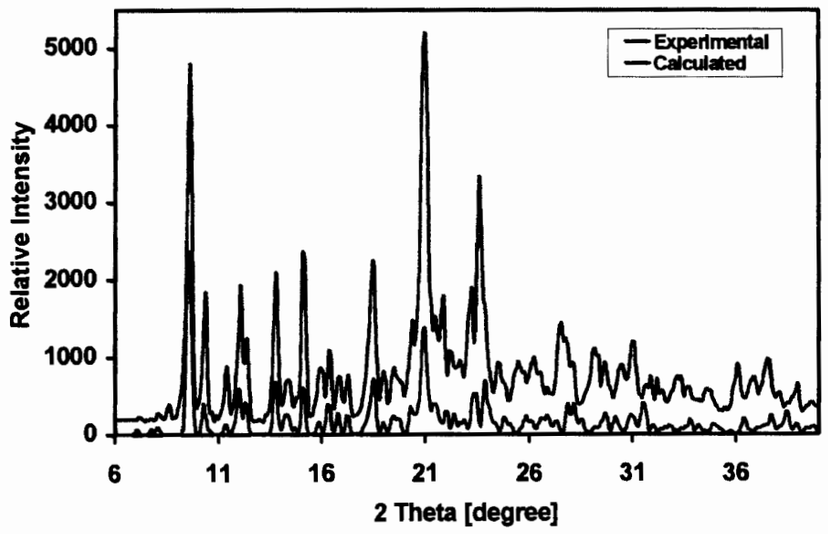

Figure 4.8 Experimental and Calculated XRD patterns for COTMB

4.7 REFERENCES

1. G. M. Sheldrick, *Acta Cryst.*, 1990, **A46**, 467.

2. G. M. Sheldrick and E. Egert, *Acta Cryst.*, 1985, **A41**, 262.

3. V. J. Griffith, *Physicochemical Characterisation of Cyclodextrin-Drug Complexes*, PhD Thesis, University of Cape Town, 1996.

4. G. M. Sheldrick, SHELXL-93, *Program for the Refinement of Crystal Structures*, University of Göttingen, Germany, 1993.

5. W. Saenger, *Inclusion Compounds*, Volume 2, Chapter 8, London, Academic Press, eds., J. L. Atwood, J. E. D. Davies and D. D. MacNicol, 1994.

6. C. H. L. Kennard, G. Smith and A. H. White, *Acta Cyst.,* 1982, **B38,** 868.

7. K. Yvon, W. Jeitschko and E. Parthe, *J. Appl. Crystallogr.*, 1977, **10**, 7.

CHAPTER FIVE

CHAPTER 5: TRIMEB COMPLEX OF CLOFIBRATE

5.1 INTRODUCTION

Clofibrate (ethyl-2-(4-chlorophenoxy)-2-methylpropionate) (II) is an ester derivative of clofibric acid. This compound is poorly water-soluble, bitter tasting and oily. The boiling point of clofibrate is 148-150 °C. Like clofibric acid, clofibrate is also an anti-hyperlipoproteinemic drug and is used for the treatment of some forms of hyperlipidaemia. In vivo studies showed that clofibrate is hydrolysed to clofibric acid and it is believed that clofibric acid is the active metabolite.[1]

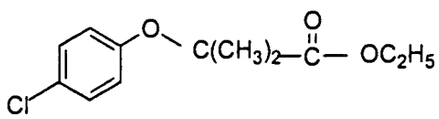

II

Clofibrate is sensitive to photo-oxidation. The photochemical stability of clofibrate and its CD complexes were studied by Uekama et al.[2] These authors suggested that the photodegradation of clofibrate in β- and γ–CD is much lower than that of the pure drug, indicating prolonged storage time for complexed drugs. Therefore, the fact that complexation might reduce the extent of photochemical reaction is advantageous. Cyclodextrin complexation of clofibrate also serves as an advantage in that the liquid guest compound can be transformed into solid complexes, making them suitable for tabletting. Anguiano-Igea et al.[3] have characterised the β-CD inclusion complex of clofibrate using XRD, DSC and IR spectroscopy. These authors also carried out dissolution rate studies which showed that the clofibrate entrapped in the inclusion complex dissolved much faster than uncomplexed liquid clofibrate.

Recently Anguiano-Igea et al.[4] in a separate publication reported NMR studies of the β-CD clofibrate inclusion compound, where it was suggested that the host-guest interactions in the complex are predominantly hydrophobic in nature occurring between the clofibrate phenyl ring and the interior of the β-CD cavity. These NMR data were also used to generate a three-dimensional model of the inclusion complex and it was suggested that the guest chlorophenyl ring is inserted in the CD cavity from the secondary side of the macrocycle while the isopropionate side chain of clofibrate protrudes from the primary end of the β-CD molecule.

5.2 PREPARATION OF COMPLEXES

The Trimeb complex of clofibrate was prepared by kneading equimolar amounts of Trimeb and clofibrate with a minimum amount of ethanol using a mortal and pestle. The kneaded complex was then recrystallised from water to yield single crystals which were later used for single crystal X-ray analysis. The complex will be referred to as CETMB.

5.3 THERMAL ANALYSIS

The TG-DSC traces of CETMB are shown in Figure 5.1. The TG trace shows a 1.1 % mass loss in the temperature range 30 to 70 °C, which is equivalent to exactly one water molecule per Trimeb molecule. Dehydration is evident as endotherm A in the DSC trace. The anhydrous CETMB complex melts at 140 °C, represented by endotherm B on the DSC trace. This is similar to the behaviour of the Trimeb complex of ibuprofen reported earlier.[5]

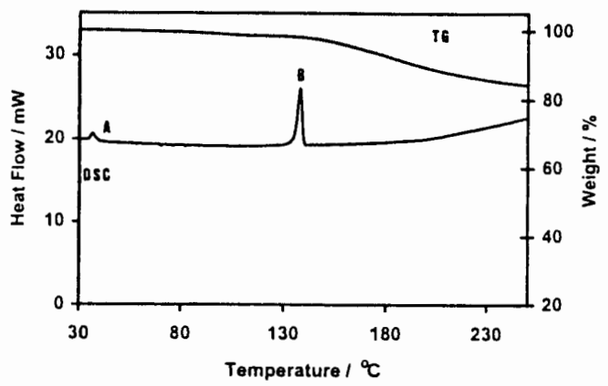

Figure 5.1 TG-DSC trace for CETMB complex

5.4 SINGLE CRYSTAL ANALYSIS

5.4.1. DATA-COLLECTION

X-ray diffraction data were collected on a Nonius Kappa CCD diffractometer using graphite-monochromated MoKα radiation generated at 50kV and 30mA. A crystal of 0.45 x 0.35 x 0.25mm was mounted on a glass fibre. The data were first collected at 293K but following refinement of the host molecule, the guest molecule could not be resolved from the difference electron density maps. It was then decided to collect the data at lower temperature (173K) by cooling the crystal continuously in a stream of nitrogen vapour from an Oxford Cryostream. The mounted crystal was inserted into a Lindemann capillary. This was necessary in order to minimise exposure to condensation from the atmosphere. Details of the data-collection strategy are listed in Table 5.1.

5.4.2 STRUCTURE DETERMINATION AND REFINEMENT

The crystal structure of CETMB was solved by the isomorphous replacement method using co-ordinates of the non-hydrogen atoms (excluding O(6), C(7), C(8) and C(9) atoms) of the host Trimeb in the isomorphous Trimeb complex of (S)-naproxen.[6] The structure was refined by full-matrix least-squares refinement using the SHELXL-93 program[7] with subsequent location of the remaining non-hydrogen atoms of the host and guest molecules from the electron density map. Hydrogen atoms bonded to the carbon atoms of both host and guest were inserted in idealised position (C-H bond length of 0.98Å) and their separately assigned common variable isotropic temperature factors were allowed to refine freely. All non-hydrogen atoms of the guest molecule were clearly resolved and refinement of these atoms proceeded satisfactorily. The guest phenyl ring was modelled as a rigid hexagon. Toward the end of the refinement, the expected single water molecule was sought in a difference electron density map. The most prominent peak had an acceptable electron density of approximately 2 $eÅ^{-3}$ and refined successfully when assigned a scattering factor of oxygen. However, subsequent inspection of geometric parameters showed this peak to be unacceptably close (2.37(1)Å) to a carbon atom of the guest molecule (C(10)). The peak was accordingly excluded from the refinement. No other prominent peak appeared in the map and it was concluded that the single water molecule was probably disordered over more than one crystallographic site. Final fractional co-ordinates for all atoms of the CETMB complex are given in Appendix A on the appended diskette in ASCII format under the filename CETMB.TEX.

Appendix B, also on diskette gives a full listing of observed (F_o) and calculated (F_c) structure factors. These are given under the filename CETMB.SFT.

5.4.3 HOST-GUEST INTERACTION AND CRYSTAL PACKING

The numbering scheme of clofibrate is shown in Figure 5.2 and that of the methyl glucose moiety is shown in Figure 4.3 (previous chapter). The oxopropionate chain of clofibrate is inserted into the Trimeb cavity from the O(2), O(3) side as shown in Figure 5.3. The oxopropionate chain conforms to the shape of the macrocylic cavity by bending toward the chlorophenyl ring (see Figure 5.4).

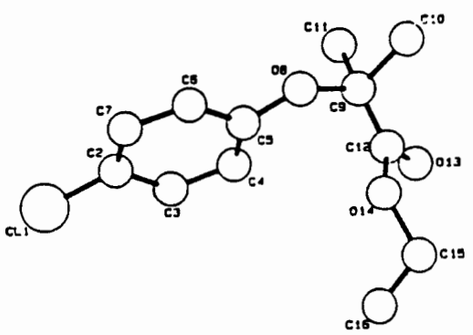

Figure 5.2 The numbering scheme and conformation of the clofibrate molecule in the complex. Only the non-hydrogen atoms are illustrated for clarity

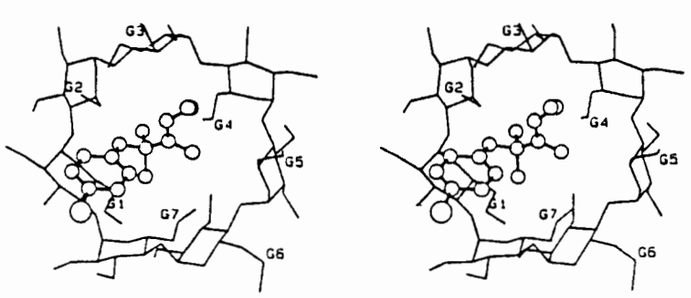

Figure 5.3 Stereodiagram of the complex CETMB: A view into cavity from the O(2), O(3) side

Table 5.1 Data-collection and refinement details for CETMB

Molecular formula	$C_{63}H_{112}O_{35}\cdot C_{12}H_{15}O_3Cl\cdot 1H_2O$
M_r/gmol^{-1}	1690.2
Crystal system	Orthorhombic
Space group	$P2_12_12_1$
Z	4
a(Å)	15.01(1)
b(Å)	21.49(1)
c(Å)	27.70(1)
V(Å^3)	8932(4)
D_c(gcm^{-3})	1.257
Crystal dimensions (mm)	0.45x0.35x0.25
T/K	173
F(000)	3632
Initial settings	
ω (°)	180
Detector to crystal distance (mm)	45
Number of frames via ϕ	366
Δϕ scans(°)	1
Exposure time (s)	177
Range scanned θ(°)	1.2≤θ≤28.3
Index range	h:0,19; k:0,28; l:0,36
Reflections collected	11486
Unique reflections	11486
Reflections with I>2σ(I)	7452
L.S. Parameters	906
R_1(I>2σ(I))	0.1249
wR_2	0.3310
S	1.058
$(\Delta\rho)_{max}$final (eÅ^{-3})	2.01
$(\Delta\rho)_{min}$ final (e Å^{-3})	-1.10

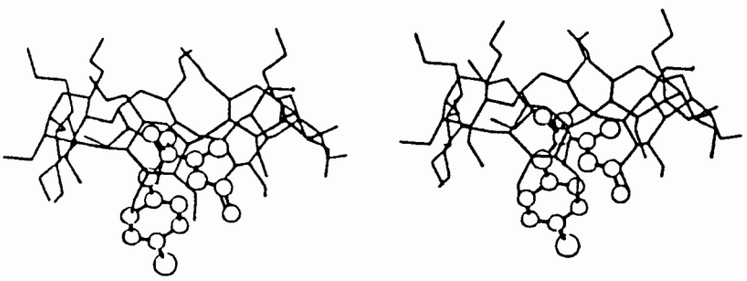

Figure 5.4 Stereodiagram of the complex CETMB: a view perpendicular to the host axis

The chlorophenyl ring makes a dihedral angle of 113° with the least-squares plane through the O(4) atoms of the host molecule. The host-guest interaction is predominantly hydrophobic in nature. There are no intermolecular hydrogen bonds between host and guest. These observations are consistent with the mode proposed by Anguiano-Igea et al.[4] based on NMR data of the β-CD complex of clofibrate. However, whereas these authors proposed that the chlorophenyl ring residue inserts into the β-CD cavity, the present study revealed that with Trimeb as host, the chlorophenyl ring protrudes from the secondary side and the side chain preferentially inserts into the cavity. Figure 5.5 shows space-filling diagrams for CETMB, which reveal how the guest molecule is buried in the cavity.

The crystal packing arrangement of the CETMB complex is shown in Figure 5.6. The host molecules are packed in a head-to-tail packing mode, forming a screw channel structure parallel to the b-axis. This packing arrangement is similar to that of the isomorphous Trimeb complexes of (S)-naproxen[6] and ibuprofen.[8]

(a)

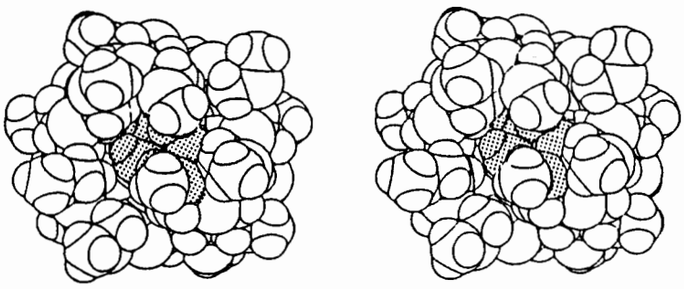

(b)

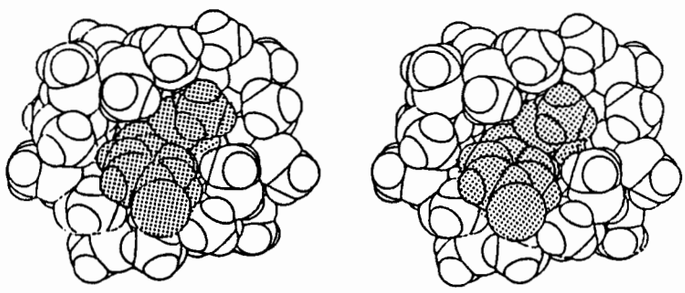

(c)

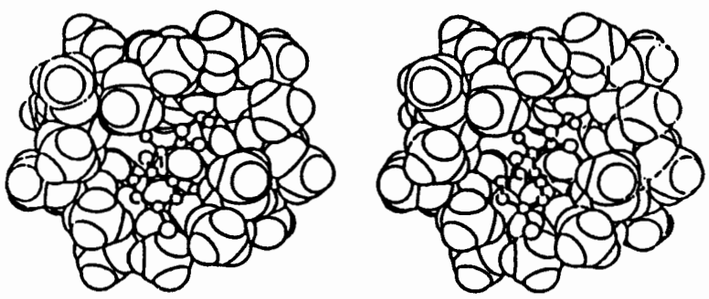

Figure 5.5 Space-filling diagrams of the CETMB complex. A view from (a) the O(6) side of the host, (b) the O(2), O(3) side of the host, and (c) the stick representation of the guest in (b)

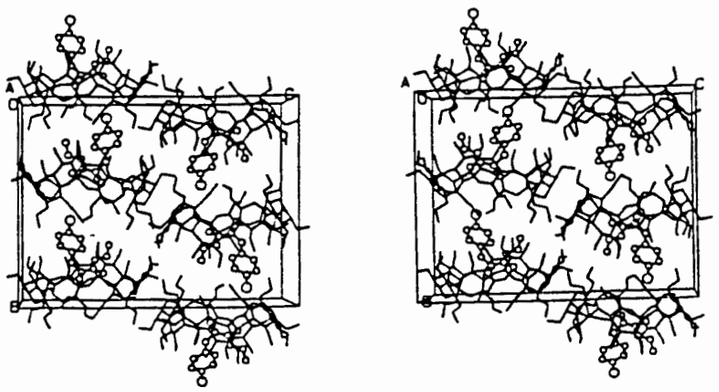

Figure 5.6 Packing diagram for the CETMB complex. Selected molecules are included for clarity

5.4.5 CONFORMATION OF THE HOST MOLECULE

All seven tri-methylated glucose residues of the Trimeb molecule in the CETMB complex are in the $^4C_1$ chair conformation. The C(6)-O(6) bonds of the G2, G4 and G7 glucose units have a (+)-*gauche* conformation while those of G3, G5 and G6 have a (-)-*gauche* conformation. The geometric parameters of the Trimeb molecule are listed in Table 5.2. The average distance of the O(4) atoms from the centre of the macrocycle is 5.19Å. The O(4) atoms of the host molecule deviate significantly from planarity as indicated in Table 5.2. Due to the absence of possible hydrogen bond donor atoms in the Trimeb molecule, it does not have the round shape characteristic of the β-CD molecule. This results in large tilt angles between the methyl glucose moieties and the least-squares plane through the O(4) atoms, which in turn results in a cup-shaped structure for the Trimeb molecule. The intramolecular C-H···O bonds play a role in partially maintaining the conformation of the macrocycle.

These are mainly the $C(6G_n)$-H···$O(5G_{n-1})$ interactions, which are listed in Table 5.3.

Table 5.2 Geometric data for the Trimeb molecule in CETMB

The glycosidic oxygen angle $C4G_n$-$O4G_n$-$C1G_{n+1}$ (°) and the torsion angle index (°)

C(1G1)-O(4G2)-C(4G2)	119.1(6)	G1	124.4
C(1G2)-O(4G3)-C(4G3)	117.4(6)	G2	139.0
C(1G3)-O(4G4)-C(4G4)	116.6(7)	G3	111.2
C(1G4)-O(4G5)-C(4G5)	118.4(6)	G4	134.8
C(1G5)-O(4G6)-C(4G6)	118.5(6)	G5	124.9
C(1G6)-O(4G7)-C(4G7)	116.5(6)	G6	124.8
C(1G7)-O(4G1)-C(4G1)	116.2(5)	G7	143.3

Glucose unit	Tilt angle (°)	Radius of heptagon (Å)	$O(4G_n)$ ···$O(4G_{n+1})$ (Å)	Deviation (Å)
G1	27.8(2)	5.44(1)	4.45(1)	0.364(5)
G2	14.7(3)	5.19(1)	4.27(1)	0.199(5)
G3	-12.0(3)	5.04(1)	4.50(1)	-0.596(6)
G4	44.7(2)	5.29(1)	4.26(1)	-0.115(7)
G5	36.3(2)	5.20(1)	4.19(1)	0.555(5)
G6	-19.8(1)	5.15(1)	4.47(1)	-0.340(6)
G7	34.4(2)	4.82(1)	4.84(1)	-0.413(6)

All parameters are defined in section 1.5.2.1

Table 5.3 Intramolecular C-H···O hydrogen bonds in CETMB

			Distance (Å)			Angle(°)
C	**H**	**O**	**C···O**	**C-H**	**H···O**	**C-H···O**
C(6G1)	H(6G1A)	O(5G7)	3.22(1)	0.98(1)	2.61(1)	121.3(9)
C(6G2)	H(6G2B)	O(5G1)	3.39(1)	0.97(1)	2.54(1)	147.7(9)
C(1G3)	H(1G3)	O(3G4)	3.11(1)	0.97(1)	2.46(1)	123.8(8)
C(6G3)	H(6G3A)	O(5G2)	3.21(1)	0.97(1)	2.51(1)	128.9(9)
C(1G5)	H(1G5B)	O(6G5)	3.25(1)	0.98(1)	2.51(1)	132.3(8)
C(6G5)	H(6G5A)	O(5G4)	3.14(1)	0.98(1)	2.44(1)	129.2(1)
C(6G6)	H(6G6A)	O(5G5)	3.17(1)	0.97(1)	2.65(1)	134.2(8)

5.4.5. CONFORMATION OF THE GUEST MOLECULE

The conformation of clofibrate in CETMB is somewhat similar to that of complexed and uncomplexed clofibric acid (see section 4.5.5). Clofibrate is liquid at room temperature and no crystal structure of low temperature forms have been published.[9] The crystal structure of CETMB has therefore enabled elucidation of the structure of clofibrate. The numbering scheme of clofibrate is given in Figure 5.2. The conformation is defined by the torsion angles listed in Table 5.4. The C(4)-C(5)-O(8) and C(6)-C(5)-O(8) angles are 125.8(8) and 113.8(8)° respectively. These deviate significantly from the expected trigonal angle as in clofibric acid (see Section 4.5.5). Overall, most bond angles and distances are in good agreement with those observed in other related molecules.[9]

Table 5.4 Torsion angles (°) for the clofibrate molecule

C(6)-C(5)-O(8)-C(9)	-165(2)
C(5)-O(8)-C(9)-C(10)	177(1)
C(5)-O(8)-C(9)-C(11)	72(2)
C(5)-O(8)-C(9)-C(12)	-60(2)
O(8)-C(9)-C(12)-O(13)	147(2)
O(8)-C(9)-C(12)-O(14)	-29(2)
C(9)-C(12)-O(14)-C(15)	-171(2)
C(10)-C(9)-C(12)-O(14)	87(2)
C(11)-C(9)-C(12)-O(14)	-158(2)
C(12)-O(14)-C(15)-C(16)	-124(2)
O(13)-C(12)-O(14)-C(15)	11(2)

5.5 X-RAY POWDER DIFFRACTION

The CETMB complex was characterised by XRD as described in Section 2.6. The theoretical XRD pattern was calculated using the program LAZYPULVERIX[10] on a personal computer running under the DOS operating system. The experimental and calculated XRD patterns for CETMB are shown in Figure 5.7. Comparison of the calculated and experimental powder XRD patterns for CETMB shows that both peak positions and relative intensities are in good agreement. This demonstrates that the sample used for the powder XRD analysis is of high purity.

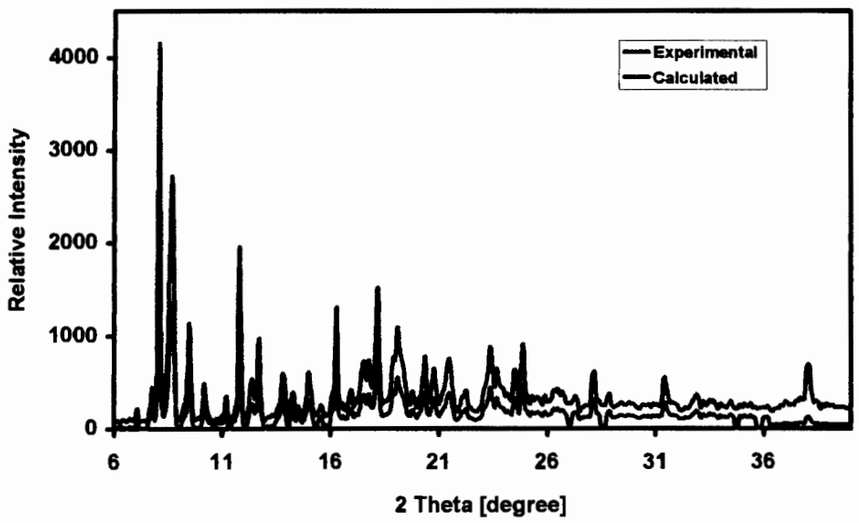

Figure 5.7 Calculated and experimental XRD patterns for CETMB

REFERENCES

1. M. M. A. Hassan and A. A. Elazzouny, *Anal. Prof. Drug Substances*, Vol 11, Academic Press New York, 1982.

2. K. Uekama, K. Oh, M. Otagiri and M. Tsuruoka, *Pharm. Acta. Helv.*, 1983, **58**, 338.

3. S. Anguiano-Igea, F. J. Otero-Espinar, J. L. Vila-Jato and J. Blanco-Méndez, *Int. J. Pharm.*, 1996, **135**, 161.

4. S. Anguiano-Igea, F. J. Otero-Espinar, J. L. Vila-Jato and J. Blanco-Méndez, Eur. J. Pharm. Sci., 1997, **5**, 215.

5. G. R. Brown, V. J. Griffith, M. R. Caira and L. R. Nassimbeni, *J. Incl. Phenom.*, 1996, **25**, 141.

6. V. J. Griffith, M. R. Caira, L. R. Nassimbeni and B. van Oudtshoorn, *J. Incl. Phenom.*, 1995, **20**, 277.

7. G. M. Sheldrick, SHELXL-93, *Program for the Refinement of Crystal Structures,* University of Göttingen, Germany, 1993.

8. G. R. Brown, *The Physicochemical Characterisation of Cyclodextrin Inclusion Compounds with Non-Steroidal Anti-Inflammatory Drugs,* MSc Thesis, University of Cape Town, 1997.

9. Cambridge Structural Database and Cambridge Structural Database System, version 5.16, October 1998, Cambridge Crystallographic Data Centre, University Chemical Laboratory, Cambridge, England.

10. K. Yvon, W. Jeitschko and E. Parthe, *J. Appl. Crystallogr.*, 1977, **10**, 73.

CHAPTER SIX

CHAPTER 6: CYCLODEXTRIN INCLUSION OF BENZODIAZEPINES

6.1 INTRODUCTION

There is an increasing interest in studying CD inclusion complexes of drugs of the benzodiazepine family.[1-4] These drugs possess a range of biological activities, most of which involve interactions with the nervous system receptors. Two benzodiazepine drug molecules were chosen to be studied in this project as possible guests for CD inclusion. They are alprazolam, 8-chloro-1-methyl-6-phenyl-4H-[1,2,4]triazolo[4,3-a][1,4] benzodiazepine (III), which is an anxiolytic drug, and midazolam, 8-chloro-6-(2-fluorophenyl)-1-methyl-4H-imidazo[1,5-a][1,4]benzodiazepine (IV), which is an anaesthetic drug.

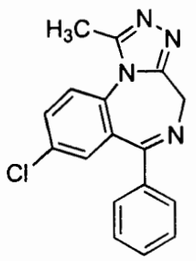

III

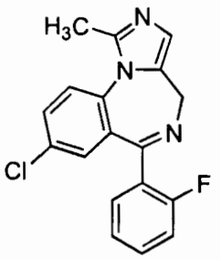

IV

Most of the benzodiazepine drugs have a very low aqueous solubility.[1] A number of chemical investigations have been carried out on the inclusion complexes of benzodiazepines with the aim of increasing bioavailability and changing the spectrum of pharmaceutical activity. Some of the benzodiazepines studied are chlordiazepoxide,[1] gidazepam,[1] cinazepam,[1] and nitrazepam[4] with β-CD and γ-CD using IR spectroscopy,

thermal analysis and X-ray diffractometry. Studies in aqueous solution which were carried out by Uekama et al.[2] and Abdel-Rahman et al.[3] revealed the magnitude of host-guest interaction between several benzodiazepines and α-, β-, and γ-CD. These authors independently found that the stability constant of the CD complexes with benzodiazepines generally increase in the order α- < γ- < β-CD, suggesting that in aqueous media the size of the cavity of β-CD most favourably accommodates the benzodiazepine molecules.

One- and two-dimensional ^{1}H-NMR studies of the inclusion compounds of gidazepam and cinazepam with β-CD have revealed that the phenyl ring of gidazepam and the *o*-chlorophenyl ring of cinazepam are inserted into the β-CD hydrophobic cavity.[1] Based on the NMR data for gidazepam[1] and cinazepam,[1] it is expected that the formation of CD inclusion compounds of alprazolam could involve the insertion of the phenyl ring into the CD cavity while the fluorophenyl ring of midazolam could be inserted in the cavity. Nevertheless, this can only be ascertained by elucidating the structures of such complexes.

In this chapter we report the results of solubility studies of alprazolam and midazolam in β-CD, Rameb (randomly methylated β-CD) and 2-hydroxypropyl β-CD (2-HPβ-CD) solutions, attempts to prepare solid complexes and the crystal structure of midazolam sesquihydrate.

6.2 SOLUBILITY STUDIES

6.2.1 METHODOLOGY

The phase solubility studies for midazolam were carried out at pH 7, pH 5.8 and pH 4 using RAMEB and 2-HPβ-CD as solubilising agents. This was necessary to assess the effect of pH on the solubility enhancement capacity of CDs on midazolam. Studies for alprazolam were carried out in de-ionised water using Rameb, 2-HPβ-CD and β-CD as solubilising agents. RAMEB and 2-HPβ-CD stock solutions of various concentrations in the range 15 to 200 mg ml^{-1} were prepared. Stock solutions of β-CD were in the range 2 to 18 mg ml^{-1}. Aliquots (5 ml) of the prepared CD solutions were individually pipetted into 25 ml stoppered flasks. Excess amounts of drugs were added to fixed volumes (5 ml) of solubility medium containing various concentrations of cyclodextrin solutions. The tightly stoppered flasks were then shaken using a Shake-O-Mat Labotec shaker at 220 rpm at room temperature for 48 h. The solutions were filtered through a 0.22 μm filter and the drug concentrations in the filtrates were determined by UV spectrophotometry on a Philips PU8700 UV/vis spectrophotometer.

6.2.2 PHASE DIAGRAMS AND STABILITY CONSTANTS FOR MIDAZOLAM

The results of the phase solubility studies for midazolam in RAMEB and HPBCD solution are shown graphically in Figures 6.1 (pH 4), 6.2 (pH 5.8) and 6.3 (pH 7) . The Rameb-midazolam curves show an A_p type behaviour at all pH values, while 2-HPβ-CD-midazolam curves show A_p behaviour at pH 7 and A_L behaviour at pH 5.8 and 4.

At any given pH, RAMEB showed a higher solubilising effect on midazolam compared to 2-HPβ-CD.

The stability constants for the A_L sytems were calculated by using equation 6.1.[5]

$$K_{11} = \frac{m}{[S_o](1-m)} \qquad 6.1$$

and that of the A_P systems by:

$$\frac{[S_t]-[S_o]}{[L_t]} = K_{11}[S_o] + K_{11}K_{12}[S_o][L_t] \qquad 6.2$$

where m = the slope of the phase solubility curve, $[S_o]$ = concentration of drug in pure buffer solution, $[S_t]$ = the concentration of the drug in different CD solutions, $[L_t]$ = CD concentration, K_{11} and K_{12} are the stability constants.

The graph of $\frac{[S_t]-[S_o]}{[L_t]}$ vs. $[L_t]$ yields a y-intercept which is equal to $K_{11}[S_o]$ while the slope is equal to $K_{11}K_{12}[S_o]$. Table 6.1 shows solubility data for midazolam in both RAMEB and 2-HPβ-CD.

Table 6.1: Solubility data for midazolam in RAMEB and 2-HPβ-CD

Host	pH	Enhancement factor [a]	Diagram type	Stability constant [M^{-1}]	
RAMEB	pH 4.0	23	A_P	K_{11} 26.7	K_{12} 0.03
2-HPβ-CD	pH 4.0	7	A_L	K_{11} 49.7	-
RAMEB	pH 5.8	200	A_P	-	-
2-HPβ-CD	pH 5.8	47	A_L	K_{11} 356.9	K_{12} 0.01
RAMEB	pH 7.0	490	A_p	-	-
2-HPβ-CD	pH 7.0	96	A_p	K_{11} 332.1	K_{12} 0.01

[a] solubility of drug in 20g/100ml CD solution divided by solubility in buffer solution only

The solubilising power of Rameb at higher Rameb concentration is barely affected by pH. As a result the solubility enhancement factor of midazolam increases with increase in pH.

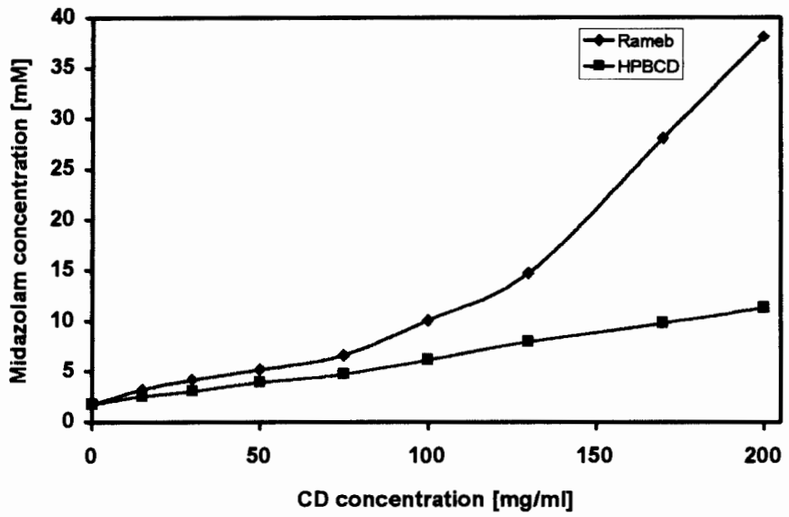

Figure 6.1 Phase solubility diagrams for midazolam in Rameb and 2-HPβ-CD at pH 4

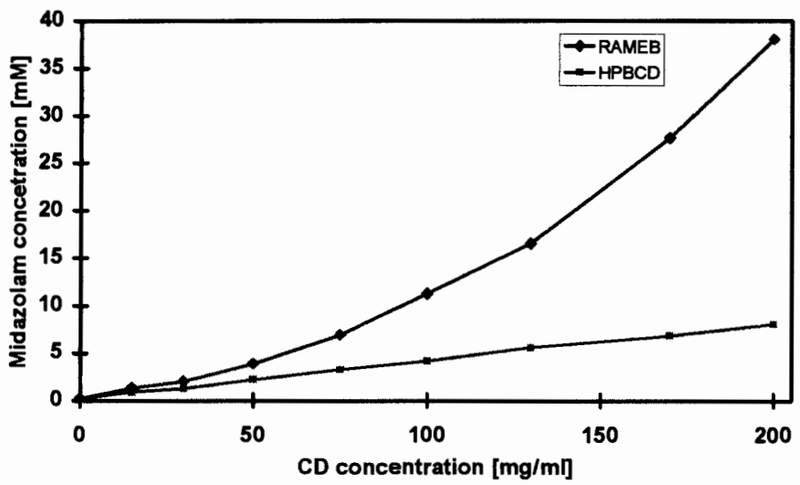

Figure 6.2 Phase solubility diagrams for midazolam in Rameb and 2-HPβ-CD at pH 5.8

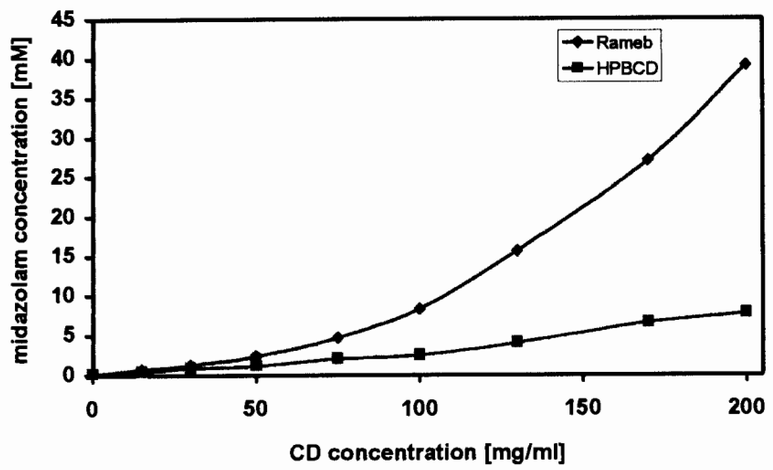

Figure 6.3 Phase solubility diagrams for midazolam in Rameb and 2-HPβ-CD at pH 7

These diagrams (Figures 6.1 to 6.3) indicate that the complexes formed are highly soluble in water and suggest that attempted preparation of Rameb and 2-HPβ-CD complexes of midazolam at pH 4, 5.6 and 7 by co-precipitation is unlikely to yield solid complexes.

6.2.3 PHASE DIAGRAMS AND STABILITY CONSTANTS FOR ALPRAZOLAM

The phase solubility diagrams for Rameb- and 2-HPβ-CD-alprazolam are shown in Figure 6.4 and for the β-CD-alprazolam system in Figure 6.5. Both Rameb-alprazolam and 2-HPβ-CD-alprazolam curves show an A_L type behaviour in de-ionised water, while the β-CD-alprazolam curve resembles a B_S type curve. Table 6.2 shows solubility data as well as stability constants for Alprazolam in β–CD, Rameb and 2-HPβ-CD. Evidently there is a stronger host-guest interaction between Rameb and alprazolam than between 2-HPβ-CD and alprazolam as reflected in Table 6.2 below.

Table 6.2: Solubility data and stability constants for Alprazolam in β–CD, RAMEB and 2-HPβ-CD.

Host	Enhancement factor [a]	Diagram type	Stability constant [M^{-1}]
β-CD	2.3	B_s	-
RAMEB	34	A_L	K_{11} 228(5)
2-HPβ-CD	16.7	A_L	K_{11} 131(4)

[a] solubility of drug in 20g/100ml Rameb or 2-HPβ-CD solution divided by solubility in pure de-ionised water. In the case of β-CD 1.8mg/100ml solution was used.

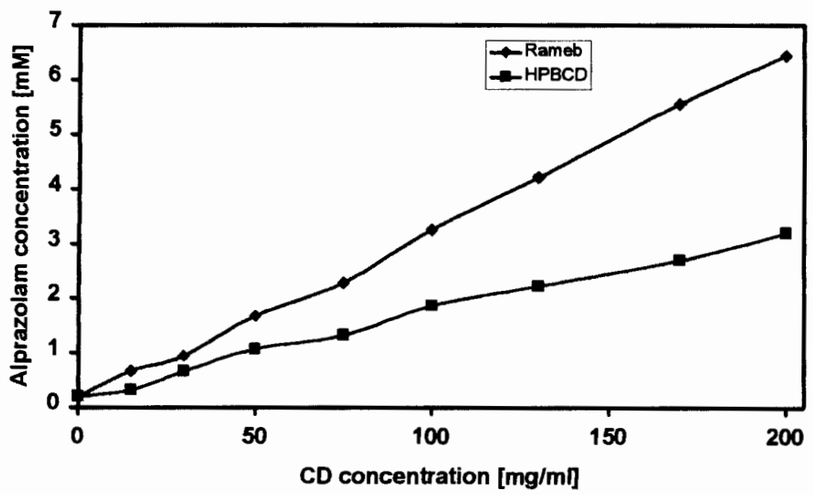

Figure 6.4 Phase solubility diagrams for alprazolam in Rameb and 2-HPβ-CD solutions

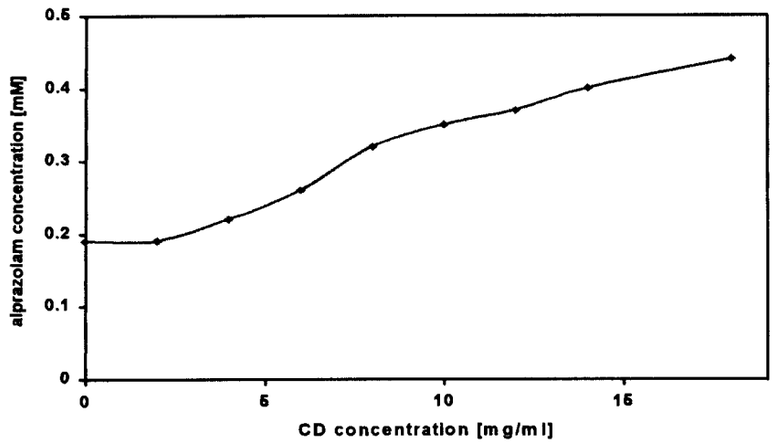

Figure 6.5 Phase solubility diagram for alprazolam in the β-CD solution

6.3 CD COMPLEXES OF BENZODIAZEPINES

In this study, preparations of β-CD, γ-CD and Trimeb complexes of alprazolam as well as midazolam by the following co-precipitation methods were attempted:

- Method A: drugs were added to a CD solution (1:1 molar ratio drug : CD) and the mixture was stirred for 36 h at 65 °C.
- Method B: drugs were pre-dissolved in a minimum amount of hot ethanol (at 65 °C). The drug-ethanol solution was then added to a CD solution and was stirred for 36 h at 65 °C.
- Method C: equimolar amounts of drugs were added to hot CD solutions, followed by the addition of 0.2 M HCl dropwise until the drug dissolved completely. The solution was stirred for 24 h followed by dropwise addition of 0.2M NaOH.

All solutions were filtered with a 0.45μm filter with the aim of growing single crystals. During the course of the attempted preparation of CD complexes, crystals formed by methods A and B were analysed by UV, DSC and TG, but were found to be CD hydrates.

The attempted preparation of the β-CD complex of midazolam by method C produced crystals of the hydrates of midazolam and β-CD. The midazolam hydrate crystallised out much faster (within 6 hours) than β-CD hydrate. The midazolam hydrate was characterised by thermal analytical methods and the results are discussed in section 6.4. Since no crystal structure of midazolam has been reported,[6] it was decided to carry out complete single crystal X-ray analysis. Knowledge of the conformational features of midazolam was also considered to be useful for future studies aimed at modelling the inclusion of midazolam in cyclodextrins.

6.4 THERMAL ANALYSIS OF MIDAZOLAM SESQUIHYDRATE

Figure 6.6 shows DSC and TG traces for the hydrate of midazolam. The stoichiometry was calculated from mass loss observed on the TG trace. The TG showed 7.6% mass loss from 30 to 135.9 °C, which is equivalent to 1.5 H_2O molecules per midazolam molecule. The DSC shows an endotherm A (onset temperature T_{on} = 92.7°C) which corresponds to the desorption of water, and exotherm B (T_{on} = 115.3 °C) corresponding to desorption of water and possibly a structural phase change. Endotherm C (T_{on} = 163.2 °C) corresponds to the melting of the anhydrous midazolam.

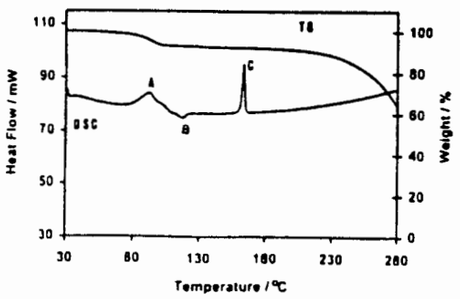

Figure 6.6 TG-DSC traces for midazolam sesquihydrate

6.5 CRYSTAL STRUCTURE OF MIDAZOLAM SESQUIHYDRATE

6.5.1 X-RAY PHOTOGRAPHY AND DATA-COLLECTION

Preliminary X-ray photography revealed Laue symmetry 2/m indicating that the compound crystallises in the monoclinic system. Conditions for observed reflections from precession photographs were *hkl h+k = 2n, h0l l=2n and 0k0 (k=2n).* These conditions indicate space groups Cc (No. 9) or C2/c (No. 15) which are non-centric and centric respectively. Intensity statistics yielded a value $|E^2-1|$ of 0.774 clearly favouring the non-centric space group. With Z = 8, this requires the asymmetric unit to contain two midazolam molecules and three water molecules.

Details of the data-collection strategy are given in Table 6.3. Data were collected in two sets. The first set of data was collected about ϕ at 1.0° scan per image in the range –222 to –40° while the second set was collected at 1.0° scan per image about ω in the range 137.7 to 100.7°.

6.5.2. STRUCTURE DETERMINATION AND REFINEMENT

The crystal structure of midazolam was solved by direct methods with program SHELXS-86[7] and refined by full-matrix least-squares with SHELXL-93.[8] In the final refinement all non-hydrogen atoms were treated anisotropically. All H atoms of midazolam were added in idealised positions and were assigned a common isotropic temperature factor.

Hydrogen atoms of the water molecules could not be located unambiguously in the difference electron density maps and are omitted in the final model. Unit cell parameters and refinement details are listed in Table 6.3. The final R-value converged to 0.075, which was satisfactory. Attempts to solve the structure in the space group C2/c were unsuccessful, thus further vindicating Cc as the correct choice. The final fractional co-ordinates for all atoms except hydrogen atoms of the water molecules are given in Appendix A on the appended diskette in ASCII format under file name MIDAZ.TEX. The observed (F_o) and calculated (F_c) structure factors are given in Appendix B, also on the appended diskette under file name MIDAZ.SFT.

Table 6.3 Data-collection and refinement details for midazolam sesquihydrate

Molecular formula	$C_{18}H_{13}N_3FCl{\cdot}1.5H_2O$
M_r/gmol^{-1}	352.8
Crystal system	Monoclinic
Space group	Cc
Z	8
a (Å)	15.45(1)
b (Å)	12.19(1)
c (Å)	19.61(1)
V (Å^3)	3425.6(1)
D_c (gcm^{-3})	1.368
Crystal dimensions (mm)	0.35x 0.30x 0.25
T/K	293(2)
F(000)	1488
Detector to crystal distance (mm)	45

Table 6.3 continued

Set 1	
Initial settings	
θ (°)	10.0
κ (°)	0.0
ω (°)	180.0
Number of frames via ϕ	182
Δϕ scans (°)	1
Set 2	
Initial settings	
ϕ (°)	-177.0
θ (°)	-10.0
κ (°)	-83.9
Number of frames via ω	62
Δω scans (°)	1
Exposure time (s)	45
Range scanned θ (°)	2.2≤θ≤26.6
Index range	h:0,9; k:0,15; l:-24,22
Reflections collected	3688
Unique reflections	3518
Reflections with I>2σ(I)	2863
L.S. Parameters	445
R_1(I>2σ(I))	0.075
wR_2	0.184
S	1.097
$(\Delta\rho)_{max}$final (eÅ^{-3})	0.77
$(\Delta\rho)_{min}$ final (e Å^{-3})	-0.59

6.5.3 CRYSTAL PACKING OF MIDAZOLAM SESQUIHYDRATE

Two midazolam molecules are in the asymmetric unit and are labelled as molecules A and B. The numbering scheme and structure of midazolam are shown in Figure 6.7. There are three water molecules present for every two midazolam molecules in the hydrate. One of the water molecules (atom O(1)) forms hydrogen bonds with the N(8A) and N(8B) atoms which are nitrogen atoms of molecule A and B. The other two water molecules are hydrogen bonded to atoms N(12) of the midazolam molecules i.e. the relevant contacts are O(2)···N(12B) and O(3)···N(12A). Atoms O(2) and O(3) are also hydrogen bonded to each other. This results in a complex intermolecular linkage between the two midazolam molecules in the asymmetric unit as shown in Figure 6.8. The hydrogen bond data are listed in Table 6.4. The packing diagram for midazolam sesquihydrate is shown in Figure 6.9. Midazolam molecules are packed in layers, forming interstitial channels which are occupied by water molecules. It is evident from Figure 6.8 that the asymmetric unit shown has C_2 pseudosymmetry. The molecular packing results in pseudo-C_2 axes running parallel to the crystal *a*-axis, which is evident in Fig 6.9.

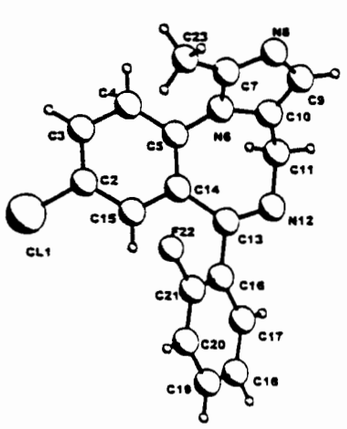

Figure 6.7 Structure and numbering scheme for the midazolam molecule.
The two independent drug molecules in the asymmetric unit have suffixes A and B added to their labels

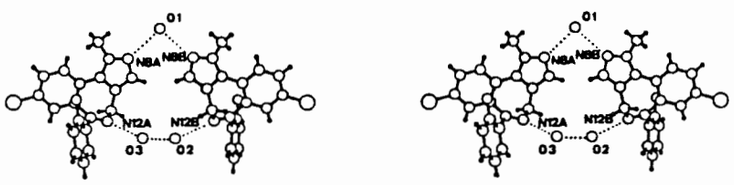

Figure 6.8 Two midazolam molecules in the asymmetric unit, linked via hydrogen bonding through water molecules

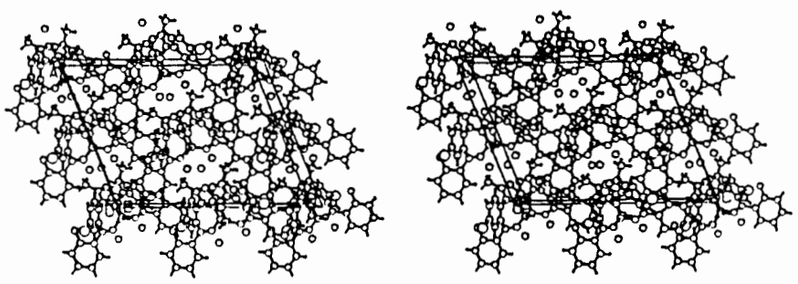

Figure 6.9 Stereopacking diagram for midazolam sesquihydrate

Table 6.4 Hydrogen bond distances

Intermolecular contact	Distance (Å)
N(8A)···O(1)	2.97(1)
N(8B)···O(1)	2.95(1)
N(12A)···O(3)	2.78(1)
N(12B)···O(2)	2.85(1)
O(2)···O(3)	2.96(1)

6.5.4 CONFORMATION OF MIDAZOLAM

Bond lengths and angles are in the expected ranges and compare favourably with those in other benzodiazepine molecules.[9-12] Selected bond lengths, bond angles, and torsion angles are listed in Table 6.5.

The seven-membered ring adopts a cycloheptatriene-like boat conformation, which is common to this class of compounds.[9] The 'boat" can be described in terms of angles between the least-squares plane through the N(6), C(10), N(12) and C(13) atoms and the 'bow' and 'stern' planes consisting of the three atoms C(10), C(11), N(12) and the set of four atoms N(6), C(5), C(14), C(13) respectively. The 'bow' and 'stern' angles for midazolam are 56.2(4) and 36.6(3)° in molecule A, and 56.5(4) and 36.6(4)° in molecule B. These values compare favourably with 56.5(7) and 35.5(3)° in 8-chloro-1-[(dimethylamino)methyl]-6-phenyl-4*H*-imidazo [1,2-*a*][1,4]benzodiazepine[11] and 55.8(6) and 36.2(6)° in 1-methyl-6-phenyl-8-(trifluoromethyl)-4*H*-1,2,4-triazolo[4,3-*a*][1,4] benzodiazepine.[12] The close correspondence between the geometrical parameters for the crystallographically independent molecules A and B (Table 6.5) suggests a fairly rigid conformation for the midazolam molecule. This merits consideration in further studies of modelling of CD-inclusion of this drug.

Table 6.5 Selected bond distances (Å), bond angles(°) and torsion angles (°)

	A	B
C(5)-N(6)	1.41(1)	1.43(1)
C(5)-C(14)	1.41(1)	1.40(1)
N(6)-C(7)	1.38(1)	1.37(1)
N(6)-C(10)	1.41(1)	1.40(1)
C(7)-N(8)	1.31(1)	1.30(1)
N(8)-C(9)	1.38(1)	1.40(1)
C(9)-C(10)	1.36(1)	1.34(1)
C(10)-C(11)	1.47(1)	1.48(1)
C(11)-N(12)	1.47(1)	1.46(1)
N(12)-C(13)	1.28(1)	1.29(1)
C(13)-C(14)	1.49(1)	1.51(1)
N(6)-C(5)-C(14)	120.5(5)	120.8(5)
C(5)-N(6)-C(10)	120.2(5)	120.9(5)
N(6)-C(10)-C(11)	120.6(5)	119.7(6)
C(10)-C(11)-N(12)	108.8(6)	109.4(6)
C(11)-N(12)-C(13)	116.9(5)	118.0(5)
N(12)-C(13)-C(14)	126.1(5)	124.3(5)
C(5)-N(14)-C(13)	122.9(5)	123.4(5)
N(6)-C(5)-C(14)-C(13)	2.4(8)	3.1(8)
C(5)-N(6)-C(10)-C(11)	43.9(8)	42.5(8)
C(14)-C(5)-N(6)-C(10)	-8.9(9)	-6.6(9)
N(6)-C(10)-C(11)-N(12)	-65.8(7)	-65.3(7)
C(10)-C(11)-N(12)-C(13)	70.5(7)	69.8(7)
C(11)-N(12)-C(13)-C(14)	-0.4(9)	1.2(8)
N(12)-C(13)-C(14)-C(5)	-45.7(8)	-46.4(8)
N(12)-C(13)-C(14)-C(15)	137.6(5)	136.1(1)
N(12)-C(13)-C(16)-C(17)	-45.9(8)	-47.1(6)
N(12)-C(13)-C(16)-C(21)	134.9(6)	133.6(1)
C(14)-C(13)-C(16)-C(17)	131.0(6)	129.1(6)
C(14)-C(13)-C(16)-C(21)	-48.3(8)	-50.2(8)

6.6 REFERENCES

1. S. A. Andronati, Y. U. E. Shapiro, L. N. Yakubovskaya, V. Ya. Gorbatyuk, K. L. Andronati, S. P. Krasnoschekaya, *J. Incl. Phenom.*, 1996, **24**, 175.

2. U. Uekama, S. Narisawa, F. Hirayama and M. Otagiri, *Int. J. Pharm.*, 1987, **16**, 327.

3. A. A. Abdel-Rahman, S. I. Saleh, G. Nakai, A. E. Aboutaleb and M. O. Ahmed, *J. Pharm. Belg.*, 1994, **49**, 23.

4. M. O. Ahmed, G. Nakai, A. E. -S. Aboutaleb, K. Yamamoto, Z. A. Rahman and S. I. Saleh, *Chem. Pharm. Bull.*, 1990, **38**, 3423.

5. T. Higuchi and K. Connors, *Adv. Anal. Chem. Inst.*, 1965, **4**,147.

6. Cambridge Structural Database and Cambridge Structural Database System, version 5.16, October 1998, Cambridge Crystallographic Data Centre, University Chemical Laboratory, Cambridge, England.

7. G. M. Sheldrick, *Acta Cryst.*, 1990, **A46**, 467-473.

8. G. M. Sheldrick, SHELXL-93, *Program for the Refinement of Crystal Structures*, University of Göttingen, Germany, 1993.

9. I. Krastanovic, N. Cvetkovic, R. Oberti and L. Karanovic, *Acta Cryst.*, 1989, **C45**, 478.

10. M. R. Caira, B. Easter, S. Honiball, A. Horne and L. R. Nassimbeni, *J. Pharm. Sci.*, 1995, **84**, 1379.

11. H. J. Butcher and T. A. Hamor, *Acta Cryst.*, 1984, **C40**, 848.

12. J. H. Kemmish and T. A. Hamor, *Acta Cryst.*, 1988, **C44**, 1823.

CHAPTER SEVEN

CHAPTER 7: CONCLUSION

7.1 CONCLUSION

In this study the following five new cyclodextrin inclusion complexes were prepared and characterized by TG, DSC, UV, IR spectroscopy, XRD and single crystal X-ray analysis:

Complex	Molecular formula
COBCD	$C_{42}H_{70}O_{35}\cdot C_{10}H_{11}O_3Cl\cdot 8.4H_2O$
COGCD	$C_{48}H_{80}O_{40}\cdot C_{10}H_{11}O_3Cl\cdot 15.5H_2O$
CODMB	$C_{56}H_{92}O_{35}\cdot C_{10}H_{11}O_3Cl\cdot 5.4H_2O$
COTMB	$C_{63}H_{112}O_{35}\cdot C_{10}H_{11}O_3Cl\cdot 1.4H_2O$
CETMB	$C_{63}H_{112}O_{35}\cdot C_{12}H_{15}O_3Cl\cdot H_2O$

The first four complexes are β-CD, γ-CD, Dimeb and Trimeb complexes of clofibric acid and the last one (CETMB) is a Trimeb complex of clofibrate. The preparations of CD complexes of clofibric acid and clofibrate were relatively straightforward. Techniques used in this study proved to be useful in confirming complex formation as well as elucidation of their structures. Thermal analysis was used more frequently and served as a principal tool to distinguish complexes from physical mixtures. Infrared spectra for COBCD, COGCD, CODMB and COTMB showed that the carbonyl stretching frequency of the complexed clofibric acid is significantly shifted to higher frequency relative to its value in the uncomplexed drug. This indicates that the C=O bond is strengthened by complex formation and that this functional group engages in new hydrogen bonds in the complexes.

The crystal structure analysis for the COBCD and COGCD complexes revealed that the included guest molecules are disordered. Such disorders are due to the linearity of the channel in COBCD, while the four-fold crystallographic symmetry causes disorder of the guest in COGCD. The packing mode of COBCD is similar to that of other β-CD complexes which crystallize in the space group C2.[1-3] COGCD crystallizes in the space group $P42_12$, which is the common space group for γ-CD complexes known thus far.[4-5]

Studies on the kinetics of dehydration of COBCD, COGCD and their corresponding host hydrates are reported in section 3.7. The magnitude of the activation energy (E_a) appeared to be related to the packing modes and the location of the water molecules in the crystals. The complexes (COBCD and COGCD) whose molecules are packed in channels, lose water more readily than the native cyclodextrin hydrates (β-CD·12.5H_2O and γ-CD·15.5H_2O) which crystallise in 'cage' packing arrangements.

The crystal structure of CODMB could not be solved by either direct or Patterson search methods using data collected as described in 4.5.1. It is therefore highly recommended that data-collection for this compound be carried out at lower temperature to improve data resolution, as this is the probable reason for the problems encountered.

In both the COTMB and CETMB complexes, the guest molecules insert from the O(2), O(3) side of the Trimeb molecule. The aliphatic chain is immersed deep in the cavity while the chlorophenyl ring protrudes from the secondary side. This mode of inclusion differs from that of native CDs where the guest aromatic ring is often inserted into the cavity. In the COTMB complex, water molecules are hydrogen bonded to the guest molecule which indeed stabilise the complex.

The elucidation of the structure of the CETMB complex is also important in that it represents the first X-ray structure determination of clofibrate, revealing one of its conformations.

Preliminary phase solubility studies were carried out on alprazolam and midazolam in Rameb and 2-HPβ-CD and revealed a significant solubility enhancement for the two species. Attempted preparation of solid cyclodextrin complexes of alprazolam and midazolam proved to be unsuccessful using various co-precipitaion methods including pH adjustment. This is expected to be the case, considering the fact that phase solubility diagrams showed a tendency toward A type behaviour. During the course of the preparation of CD complexes of midazolam using pH adjustment methods, the host and guest tend to crystallise out separately. Midazolam crystallised out as a sesquihydrate whose crystal structure was solved. The structure solution revealed that two midazolam molecules form an asymmetric unit linked by three water molecules through hydrogen bonds. This suggests that midazolam prefers to crystallize as a stable hydrate rather than forming an inclusion complex under the conditions investigated.

7.2 REFERENCES

1. I. M. Mavridis and E. Hadjoudis, *Carbohydrate Res.*, 1991, **11**, 220.

2. G. Les Bas, C. de Rango, N. Rysanek and G. Tsoucaris, *J. Incl. Phenom.*, 1984, **2**, 861.

3. C. Betzel, B. Hingerty, N. Noltemeyer, G. Weber, W. Saenger and J. A. Hamilton, *J. Incl. Phenom.*, 1983, **1**, 1181.

4. J. Ding, T. Steiner and W. Saenger, *Acta Cryst.*, 1991, **B47**, 731.

5. S. Kamitori, K. Hirotsu and T. Higuchi, *J. Am. Chem. Soc.*, 1987, **109**, 2409.

APPENDICES

Supplementary material for structures of all compounds appear on disks in Appendices A and B.

APPENDIX A

Appendix A contains

- atomic co-ordinates and equivalent isotropic displacement parameters
- bond lengths and angles
- anisotropic displacement parameters
- hydrogen atom co-ordinates
- torsion angles.

Files containing these data for the complexes are named using the abbreviation for the complexes with the extension "TEX" e.g. COBCD.TEX contains the above mentioned data for the CODMB complex. Data for midazolam sesquihydrate are stored in MIDAZ.TEX .

APPENDIX B

This contains tables of observed (F_o) and calculated (F_c) structure factors. Files containing structure factor tables for the complexes are named using the abbreviation for the complexes used in the text with extension "SFT", e.g. COBCD.SFT contains the structure factor tables for the CODMB complex. The structure factor tables for midazolam sesquihydrate are given in MIDAZ.SFT.

All files are text files and can be viewed in an editor under any of the following operating systems:

APPLE MAC

DOS

Linux

OS/2

UNIX

VMS

WINDOWS 3.1

WINDOWS 95

WINDOWS 97.